The Role of Experimental and Co-ion Specific Factors in Membrane Permselectivity

Yuanyuan Ji

B.S., Tianjin University, 2014

A Thesis presented to the Graduate Faculty
of the University of Virginia in Candidacy for the Degree of
Master of Science

Department of Chemical Engineering

University of Virginia
July, 2017

Abstract

The apparent permselectivity of an ion exchange membrane is a critical ion transport property that influences the efficiency of electric field-driven membrane technologies and often is measured using a pseudo-steady state measurement technique. This study first examined three major experimental factors that might affect the accuracy of permselectivity measurement. Among them, temperature had a small influence on apparent permselectivity properties for two commercially available membranes (i.e., Selemion CMV and CMI-7000s), as the value of apparent permselectivity decreased by approximately 2% as temperature increased from 14^{o}C to 31^{o}C. Membrane potential measurement fluctuations contributed approximately 0.2% to 0.5% uncertainty to apparent membrane permselectivity. Deviations from target sodium chloride solution concentrations of 10ppm/L introduced approximately 0.015% to 0.1 error, respectively, in apparent permselectivity. The magnitudes of these uncertainties typically are comparable to the magnitude of the measurement variability associated with disassembling and reassembling the measurement cell between replicate measurements made on the same sample, so the overall influence of the experimental factors considered in this study on apparent permselectivity is expected to be generally small.

At the same time, the permselectivity, co-ion sorption coefficient and co-ion diffusion coefficient of a lab-prepared CEM, XLAMPS was also characterized using four different salts: sodium chloride, sodium bromide, sodium nitrate and sodium perchlorate. Co-ion species were also found to intrinsically affect membrane permselectivity via both co-ion sorption and co-ion diffusion. The membrane permselectivity of XLAMPS, a lab-prepared CEM, follows the trend: $\alpha_{\mathrm{NaCl}} > \alpha_{\mathrm{NaNO_3}} > \alpha_{\mathrm{NaBr}} > \alpha_{\mathrm{NaClO_4}}$. The co-ion sorption coefficient of XLAMPS follows the

trend: $K_{\mathrm{NaClO_4}} > K_{\mathrm{NaNO_3}} > K_{\mathrm{NaBr}} > K_{\mathrm{NaCl}}$, whereas the co-ion diffusion coefficient of XLAMPS follows the opposite trend: $D^m_{\mathrm{NaCl}} > D^m_{\mathrm{NaBr}} > D^m_{\mathrm{NaNO_3}} > D^m_{\mathrm{NaClO_4}}$. These three trends, combined together, reveal a competing mechanism between co-ion sorption and co-ion diffusion in determining the relative magnitude of membrane permselectivity. The salt sorption coefficient is connected with bare co-ion radius and co-ion excess polarizability through a continuum dielectric model. According to the model, large bare co-ion radius and large co-ion excess polarizability are related with lower co-ion sorption energy barrier and higher co-ion sorption coefficient. However, for sodium perchlorate, the formation of $NaClO_4$-EO complexation contributes to its high sorption coefficient as well. The relative magnitude of salt diffusion coefficients of sodium bromide and sodium nitrate can be inversely connected with their hydrated radii. Whereas for sodium chloride and sodium perchlorate, hydrated radii might not be the only influencing factor. Repulsive interactions might exist between sodium chloride and membrane polymer matrix, and attractive interactions might exist between sodium perchlorate and the membrane polymer matrix. The former will increase salt diffusion coefficient in the membrane and the later will reduce salt diffusion coefficient in the membrane.

List of Figures

List of Tables

Acknowledgements

I would like to thank my advisor Geoff Geise for his valuable advice and inspiration on my project and also thank our group members, Tianyi Xue, Huan Zhang, Drew Biedermann, Bill Morris, Hongxi Luo, Kevin Chang, Saringi Agata, and Kevin Bahati for their support from daily experiments. I would like to than Prof. Carta's for his advice during my qualify exam, Ricky Buchanan for helping me with equipment. I would also like to thank Ni Yan, from University of Texas, for her advice on membrane preparation.

I also want to thank all my families and friends for their support, especially my parents Bin Ji and Dongdong Hu, my friend Jingjing Hao, Bo Yang. I cannot have the work done without their support.

This research was supported by start-up support at the University of Virginia. Part of this thesis were reproduced from a paper published by the author on Industry & Engineering Chemistry Research: Ji, Y.; Geise, G. M. The Role of Experimental Factors in Membrane Permselectivity Measurements. *Ind. Eng. Chem. Res.,* **2017**, *56* (26), 7559 – 7566.

Table of Contents

1. Introduction

Ion exchange membranes (IEMs) are used widely in separation and energy generation technologies, such as electrodialysis (ED) and reverse electrodialysis (RED).[1-10] In general, these processes rely on ion exchange membranes to regulate electric field-driven ion migration.[11] Cation exchange membranes (CEMs), which have negatively charged groups bound to the matrix, enable selective transport of cations in an electric field, and anion exchange membranes (AEMs), which have positively charged groups bound to the matrix, enable selective transport of anions in an electric field.[9, 11] The permselectivity of these CEMs and AEMs is a measure of how exclusively CEMs transport cations or how exclusively AEMs transport anions[10] and affects the energy efficiency of electric field-driven membrane applications. In RED, for example, the open circuit voltage of the membrane stack varies linearly with permselectivity, and the maximum power density scales with the permselectivity squared.[6, 7, 12, 13] Therefore, membranes with low permselectivity result in low RED power output.[6, 7, 14] In ED, low permselectivity result in less efficient desalination because more power mush be supplied to the system, as compared to a high permselectivity membrane, to accomplish an equivalent separation.[15, 16]

Ion exchange membrane permselectivity, α, is defined as:

$$\alpha \equiv \frac{t_{\mathrm{M}}^{\mathrm{m}} - t_{\mathrm{M}}^{\mathrm{s}}}{t_{\mathrm{X}}^{\mathrm{s}}} = 1 - \frac{t_{\mathrm{X}}^{\mathrm{m}}}{t_{\mathrm{X}}^{\mathrm{s}}} \tag{1}$$

where t_i^j is the transport number of ion *i* in phase *j*.[10, 11] Superscripts m and s refer to the membrane and solution phases, respectively. Subscripts M and X refer to counter-ions (cations in CEMs and anions in AEMs) and co-ions (anions in CEMs and cations in AEMs), respectively. Transport numbers represent the fraction of current carried by each ion in each phase.[17, 18] In a perfectly permselective membrane, only counter-ions carry current through the membrane (i.e.,

$t_{\mathrm{M}}^{\mathrm{m}} = 1$ and $\alpha = 1$). For a nonpermselective membrane, ion transport in the membrane is analogous to that in solution (i.e., $t_{\mathrm{M}}^{\mathrm{m}} = t_{\mathrm{M}}^{\mathrm{s}}$), and the permselectivity is equal to zero. It can also be concluded from the second part of right hand side of equation 1, where permselectivity is only expressed in co-ion transport numbers, that permselectivity decreases with increasing co-ion transport number in membrane phase.

The ion transport number, is then calculated through:

$$t_i^j = \frac{|z_i| C_i^j D_i^j}{\sum_j |z_j| C_j^j D_j^j} \tag{2}$$

where z_i is the ion charge, c_i^j is the concentration of ion *i* in phase *j*, D_i^j is the diffusivity of ion *i* in phase *j*.

It can be further concluded that the membrane permselectivity decreases with either increasing in co-ion concentration in the membrane, or increasing in co-ion diffusion coefficient in the membrane, by combining equation 1 with equation 2. According to equation 2, an increase in either co-ion membrane concentration or co-ion diffusion coefficient increases co-ion transport number in membrane phase, thus reducing permselectivity according to equation 1. Therefore, any factor, that facilitates co-ion partitioning into membrane phase or co-ion diffusion inside membrane phase will reduce membrane permselectivity, and vice versa. For example, IEMs with high fixed charge group concentration are typically related with high permselectivity.[13, 14] For IEMs, the co-ion sorption (i.e., partition) isotherms decreased somewhat with increasing fixed charge group concentration, presumably owing to enhanced Donnan exclusion with higher fixed charge group concentration.[19, 20]A decrease of co-ion sorption isotherms reduces co-ion concentration in the membrane phase, thus reducing co-ion transport number in membrane and ultimately increasing membrane permselectivity.

Membrane permselectivity was often measured as apparent permselectivity, as defined by Strathmann,[10, 11] using a static method. Through this method, apparent permselectivity is determined through membrane potential, E_m, that is measured while the membrane separates solutions of high, $a_{\pm}^{SL}$, and low, $a_{\pm}^{S0}$, mean electrolyte activity:

$$\alpha = \frac{\left[E_m / \left(\frac{RT}{F} ln \frac{a_{\pm}^{SL}}{a_{\pm}^{S0}}\right)\right] + 1 - 2t_M^s}{2t_X^s} \tag{3}$$

where R is the gas constant, T is the absolute temperature, and F is Faraday's constant.[10, 21] The solution concentration in each chamber of the measurement cell (Figure 1) is held constant by supplying fresh solution to the chamber, so the mean electrolyte activity of the solution in each chamber is fixed. The electric potential difference across the membrane, E_x, is measured using double junction reference electrodes. To account for asymmetry in the reference electrodes, an offset potential, E_{offset}, is measured between the two electrodes, so the membrane potential, E_m, is obtained as: [21]

$$E_m = E_x - E_{offset} \tag{4}$$

The membrane potential, E_m, can then be used to calculate the apparent permselectivity of the membrane using equation 3.

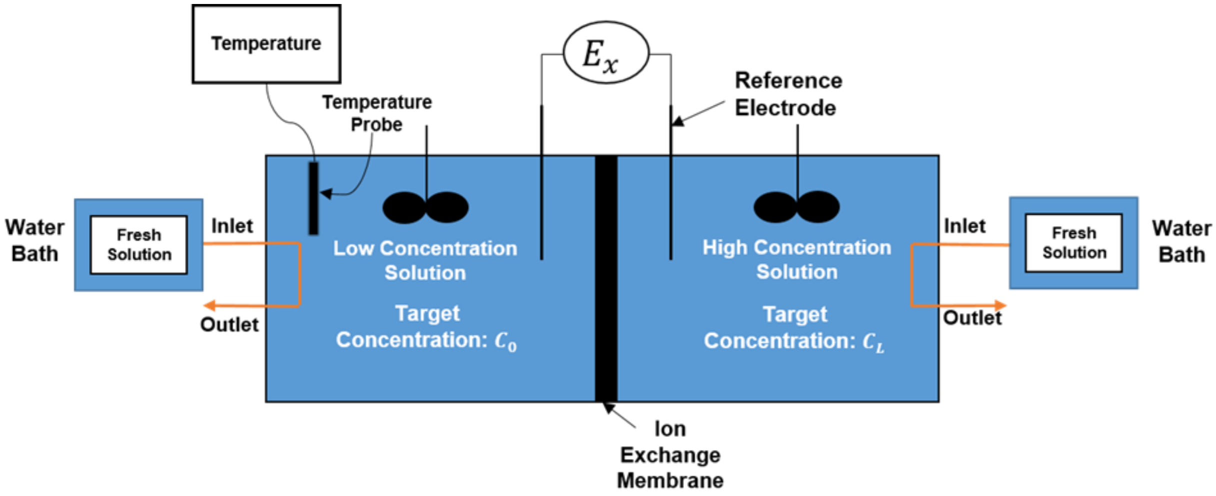

Figure 1. Schematic illustration of permselectivity measurement apparatus. The apparent permselectivity of an ion exchange membrane can be measured by placing the membrane between solutions of different salt concentration. When the concentrations of these solutions are held constant (by stirring and single pass fresh solution feeds), the electric potential difference across the membrane can be measured and ultimately related to the apparent permselectivity of the membrane. The temperature of the solutions in the cell is monitored using a temperature probe placed in the low concentration solution.

During the measurement, experimental factors such as temperature and salt concentration can potentially affect the final measured permselectivity. Here, we investigated three factors that may influence the accuracy of apparent permselectivity measurements. First, the Nernst potential calculations used to convert membrane potential measurements to permselectivity (equation 3) require a fixed temperature. Researchers often report room-temperature conditions, which may fluctuate from day to day, when measuring apparent permselectivity. Second, the mean electrolyte activity (ultimately, concentration) of the two solutions used in the measurement must be kept constant. We investigated the sensitivity of the apparent permselectivity to relevant deviations from these fixed concentrations and the effects of failing to provide a sufficiently high flow rate of fresh solution to the cell. Third, the influence of electric potential measurement fluctuations on apparent permselectivity was considered. Figure 2 illustrates these fluctuations (Characterized by ΔE) using representative data that show the electric potential difference across a membrane stabilizing as the system reaches a pseudo steady state. The standard deviation, ΔE, from the average membrane potential, E_x, can be a source of membrane permselectivity uncertainty. We report and discuss the influence of temperature fluctuations, deviations in salt concentration, and membrane potential measurement fluctuations on membrane apparent permselectivity measurements.

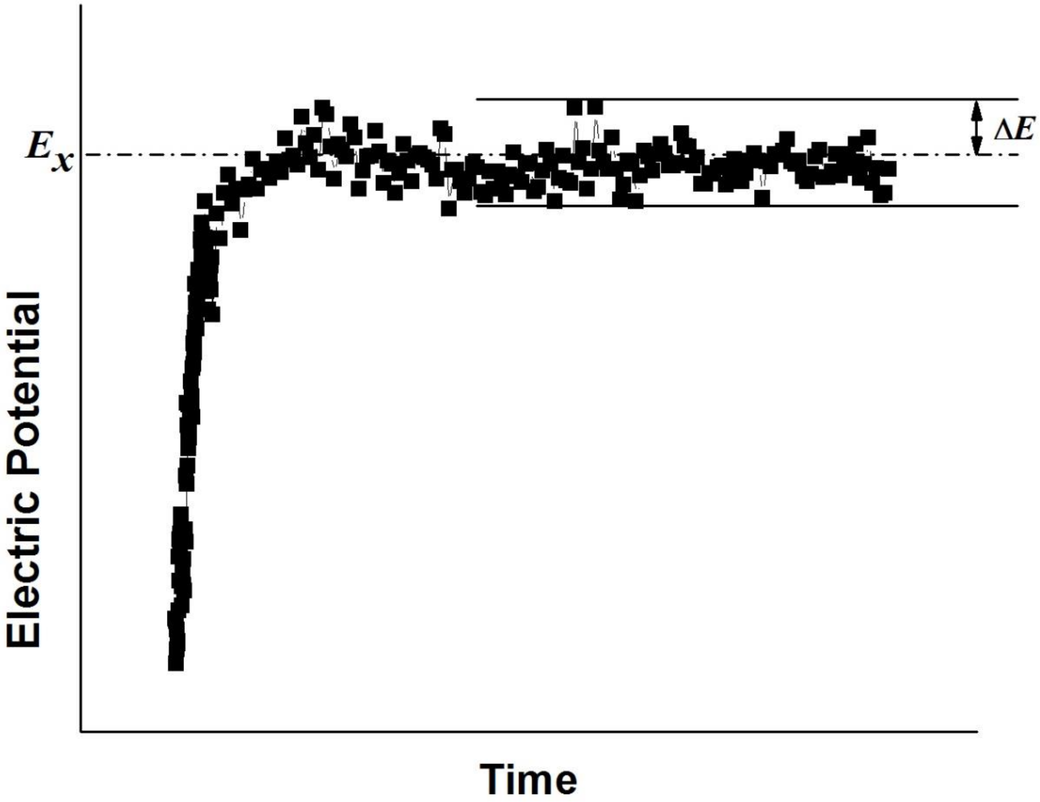

Figure 2. Representative electric potential difference, E_x, data measured, as a function of time and using reference electrodes, across a membrane that separates solutions of different salt concentration. The measured membrane potential approaches the pseudo-steady state value, E_x, and fluctuations in the measured value of E_x can be quantified as ΔE.

Besides experimental factors, the salt species used for permselectivity characterization, also influence membrane potential and permselectivity.[21-24] Furthermore, the effects of salt species on membrane permselectivity is intrinsic, as compared to only the experimental deviations brought by experimental factors. Recent work with sodium chloride and ammonium bicarbonate and two commercial membranes, by Geise et al. demonstrated experimentally that both co-ion and counter-ion identities influence membrane permselectivity for commercial CEMs and AEMs.[21] They further proposed that for Selemion AMV and CMV membranes, co-ion charge density and polarizability were related with membrane permselectivity. Co-ion with high charge density and low polarizability might lead to high permselectivity. The phenomena that different co-ion species resulted in different permselectivity were then demonstrated by our work with three other salts, other than sodium bicarbonate used by them. The permselectivity of Selemion CMV, and CMI-7000s, two commercially available membranes, were characterized by sodium chloride along with other three salts, sodium nitrate, sodium bromide and sodium perchlorate, and the results showed that different co-ion species, gave different permselectivities, as presented in Figure 3. But whether co-ion charge density and co-ion polarizability were responsible for this phenomena still remained unknown.

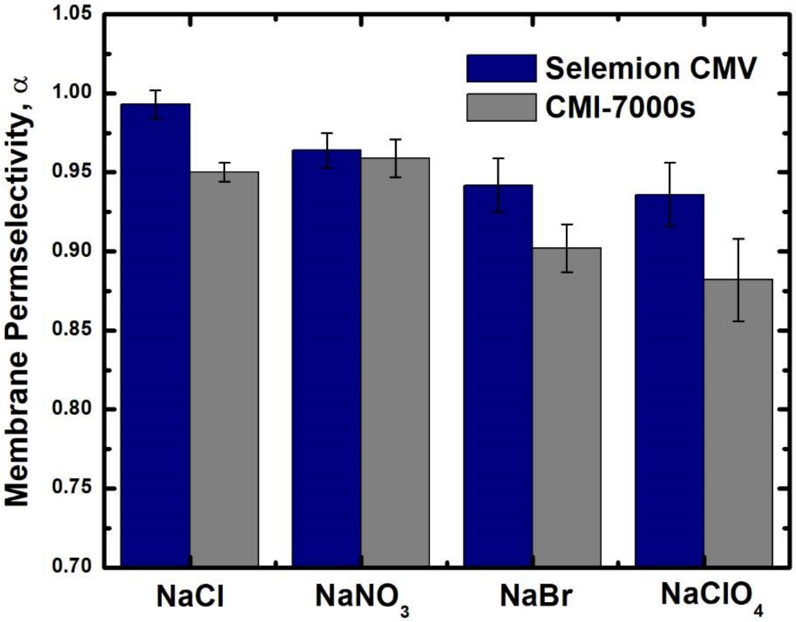

Figure 3. Apparent permselectivity of two commercially available membranes: Selemion CMV and CMI-7000s, measured with four monovalent strong salts: sodium chloride, sodium bromide, sodium nitrate and sodium perchlorate, using apparatus shown in figure 1, with salt concentrations of 0.1 mol/L and 0.5 mol/L.

Further work needs to be conducted to figure out the mechanism behind this specific co-ion effects phenomena with regard to the permselectivity of cation exchange membranes. Considering the rapid growth of more membrane-based energy generation and recovery technologies, such as vanadium flow battery and closed-loop RED, such study will be worthwhile.[21, 25, 26] In all vanadium flow battery and closed-loop RED, IEMs are exposed to many non-conventional ions such as ammonium, bicarbonate, vanadium, or bisulfite. In such case, understanding the membrane behavior in the presence of different co-ions becomes significant in improving the membrane working efficiency for those technologies.

In this study, besides experimental factors, we also seek to investigate the effect of co-ion specific factors on membrane permselectivity. The co-ion specific factors were chosen to be size and polarizability since they are two most commonly mentioned intrinsic ion specific parameters, except for valence.[27] Based on previous discussions connecting co-ion transport and permselectivity, it is then reasonable to assume that co-ion specific factors, such as charge density, radius, or polarizability, affect membrane permselectivity via co-ion sorption or co-ion diffusion. The permselectivity, co-ion sorption coefficient and co-ion diffusion coefficient of a lab-prepared CEM, XLAMPS were measured with four monovalent salts, sodium chloride, sodium bromide, sodium nitrate and sodium perchlorate. The cation was fixed as sodium, whereas the choice of these four anions allowed us to examine a typical range of ion size and polarizability. A continuum dielectric model, which was firstly proposed by Ninham et al.,[28] was applied to qualitatively predict the co-ion sorption free energy barrier, and to hopefully connect co-ion bare radius, polarizability with co-ion sorption. Mackie and Meares model was applied to predict co-ion diffusion coefficient in the membrane phase.[29-31] The sorption coefficient results of XLAMPS with sodium perchlorate, combined with previous literature,[32, 33] presumably revealed that sodium perchlorate formed complex structure with the ethylene glycol groups in XLAMPS, so the sorption coefficients of three other non-charged, lab-prepared membranes, XLPEGDA (n=3, 10, 13) were also measured to provide evidence on the formation of such complexation.

2. Materials and Methods

2.1 Materials

Two commercially available membranes were used for the study with regard to experimental factors as well as permselectivity measurements with four salts (i.e., sodium chloride, sodium bromide, sodium nitrate and sodium perchlorate). They are: Selemion CMV (Asahi Glass, Co., Tokyo, Japan) and CMI-7000s (Membranes International Inc., NJ, USA). Their ion exchange capacity (IEC), which is a measure of concentration of charged functional groups in the polymer matrix, hydrated thickness and water uptake in salt solutions were either reported by the manufacture or measured experimentally, as shown in Table 1.

Table 1. Physical properties of the commercially available polymeric ion exchange membranes considered in this study. For water uptake measurements, the membranes were initially hydrated in either 0.1 M or 0.5 M salt solutions at ambient temperature, and the uncertainty is reported as the standard deviation from the mean value of six measurements. The membrane thickness values are reported as an average and standard deviation of four to five measurements made on the as received membrane sheets. The membrane water uptake was found to be statistically indistinguishable in different salt solutions under same concentration, so only the water uptake in NaCl solutions were reported.

Membrane	Ion Exchange Capacity (IEC) [meq / g(dry polymer)]	Water Uptake [g(water) / g(dry polymer)]		Thickness of Fully Hydrated Membrane [μm]
		0.1 mol/L NaCl	0.5 mol/L NaCl	
Selemion CMV	2.08[34]	0.28±0.01	0.25±0.02	109±2
CMI-7000S	1.6±0.1[35]	0.32±0.01	0.35±0.02	590±3

Cross-linked poly (AMPS-PEGDA) (XLAMPS) and cross-linked PEGDA (XLPEGDA) membranes were used in this study for kinetic desorption measurements and were formed via free radical UV-photo-polymerization of a pre-polymerization solution. The pre-polymerization solution of XLAMPS was prepared by mixing a 50 wt% 2-Acrylamido-2-methyl-1-propanesulfonic acid sodium aqueous solution (catalog number 65582, Sigma-Aldrich, St. Louis, MO) with a crosslinker, PEGDA (average M_n=525g mol^{-1}, catalog number 437441, Sigma-

Aldrich, St. Louis, MO), and their mass ratio was controlled to be 2:3. The pre-polymerization solution of XLPEGDA were pure PEGDA (average M_n=250g mol^{-1}, catalog number 475629, average M_n=525g mol^{-1}, catalog number 437441, average M_n=700g mol^{-1}, catalog number 455008, Sigma-Aldrich, St. Louis, MO), but with varying repeating units (n=3, 10, 13). For all pre-polymerization solutions, 0.1 wt% 1-Hydroxycyclohexyl phenyl ketone, HCPK (catalog number 405612, Sigma-Aldrich, St. Louis, MO) were added as initiator.

The pre-polymerization solution was then confined between glass plates, and spacers were used between two plates to control the membrane thickness, the final hydrated thickness of all lab-prepared membranes were 200 – 500μm. The photo-polymerization of pre-polymerization solutions were performed by irradiating the mixture with 120 μJ/cm^2 254 nm UV light for 300 sec for XLAMPS and 120 sec for XLPEGDA (n=3,10,13) at room temperature.[36] The crosslinked polymers were soaked in DI water prior to use to remove any solvent or unreacted monomers. Their structures are presented in Figure 4. Their physical and chemical properties were either calculated or measured experimentally, as shown in Table 2.

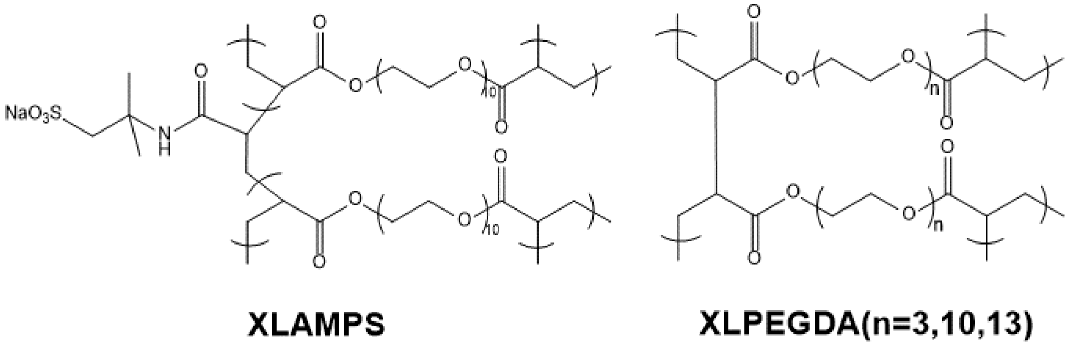

Figure 4. Schematic illustration of lab-prepared membrane structures used in this study

Table 2. Physical and Chemical Properties of lab-prepared membranes used in this study. The ion exchange capacity of XLAMPS was calculated from the amount of raw materials used in the crosslinking process. For water uptake measurements, the membranes were initially hydrated in either 0.1 M or 0.2 M salt solutions at ambient temperature, and the uncertainty is reported as the standard deviation from the mean value of six measurements. The membrane thickness values are reported as an average and standard deviation of four to five measurements made on the as received membrane sheets. The membrane water uptake was found to be statistically indistinguishable in different salt solutions under same concentration, so only the water uptake in NaCl solutions were reported. The water uptake was also found to be statistically indistinguishable in 0.1 mol/L and 0.2 mol/L NaCl solutions. So all the water uptake data points were put together to calculate the average water uptake and the partition coefficient K_w *was estimated from the average water uptake.*

Membrane	Ion Exchange Capacity (IEC) [meq / g(dry polymer)]	Water Uptake (W_u) [g(water)/ g(dry polymer)]		Dry Density (ρ_P) [g / cm^3]	Water Partition Coefficient (K_w) [g(water)/ cm^3 (swollen polymer)]
		0.1 mol/L NaCl	0.2 mol/L NaCl		
XLAMPS	1.09	0.80±0.02	0.81±0.02	1.31	0.51±0.03
XLPEGDA(n=3)	-	0.05±0.00	-	1.27	0.06±0.00
XLPEGDA(n=10)	-	0.33±0.02	-	1.21	0.29±0.02
XLPEGDA(n=13)	-	0.52±0.02	-	1.19	0.38±0.02

2.2 Methods

2.2.1 Water Uptake

The water uptake of commercial membranes were measured gravimetrically after membrane samples were equilibrated for 24 to 48 hours with 0.1 mol/L or 0.5 mol/L aqueous salt solutions at ambient temperature, and the water uptake of lab-prepared membranes were measured using the same method after membrane samples were equilibrated for 24 to 48 hours with 0.1 mol/L or 0.2 mol/L aqueous salt solutions at ambient temperature.[37] This soaking time allowed the films to fully hydrate and equilibrate with the salt solution. Then, the samples were taken out of the solution, and the wet mass was measured quickly after excess solution was wiped off the membrane surface using a laboratory wipe. The samples were dried under vacuum at ambient temperature until the dry mass of the sample stabilized. The drying time was typically between 36 and 48 hours. The dry mass was measured immediately after the drying process to prevent sorption of moisture from the atmosphere, and the water uptake W_u, of the sample was calculated as:

$$W_u = \frac{m_{wet} - m_{dry}}{m_{dry}} \tag{5}$$

where m_{wet} is the hydrated membrane mass, and m_{dry} is the dry membrane mass. Water uptake for each material was reported as the average of six measurements, and the uncertainty was taken as the standard deviation of those six measurements. The membrane water uptake of all membranes were measured in four salt solutions (i.e., NaCl, NaBr, $NaNO_3$ and $NaClO_4$) under different concentrations (i.e., 0.1 mol/L, 0.2 mol/L, or 0.5mol/L), respectively. However, the results of membrane water uptake in different salt solutions with same concentration were found to be statistically indistinguishable, so only the results in NaCl solutions were reported. Samples were discarded following the water uptake measurement.

2.2.2 Membrane Dry Density

The density measurement methodology was learned from literature.[36, 38] The density of dry polymer membranes was determined using a Mettler Toledo analytical balance (Model XSE204, Switzerland) with a Mettler Toledo density determination kit (Part #11106706). The measurements were conducted following the procedure of density determination of solid, as provided by Mettler Toledo.[39] The dry polymer membrane sample was first weighed in air, then in an auxiliary liquid, which is a non-solvent for the polymer under consideration. The polymer dry density was calculated as:

$$\rho_P = \frac{m_1}{m_1 - m_2}(\rho_2 - \rho_1) + \rho_1 \tag{6}$$

where: m_1 is the weight of sample in air, m_2 is the weight of sample in auxiliary liquid, ρ_1 is the density of air under measured temperature, ρ_2 is density of the auxiliary liquid under measured temperature. N-Heptane was chosen to be the auxiliary liquid since it was recorded to show little affinity for PEO.[38, 40] All the density measurements were conducted under ambient temperature, but the exact temperature values were still recorded by a thermometer placed in the auxiliary liquid for more precise determination of air and liquid density.

2.2.3 Membrane Potential and Apparent Permselectivity

Apparent permselectivity was measured experimentally using a two-chamber apparatus (Figure 1).[10, 21] A membrane sample was placed between the two cell chambers, and the chambers were filled with aqueous salt solutions of different concentrations. Overhead mechanical stirring at 460 rpm ensured that the solution in each chamber was well mixed without creating cavitation-induced bubbles in the chamber. Additionally, the concentration of the solutions in each chamber were maintained by a continuous, single-pass flow of fresh solution. Additionally, the concentrations of the solutions in each chamber were maintained by a continuous, single-pass flow of fresh solution. Double junction Ag/AgCl reference electrodes (RR EF 0024, Pine Instrument Company, Grove City, PA), filled with 10% KNO3 solution, were placed in the solutions on either side of the membrane. Double junction reference electrodes provided a more stable potential reading compared to single junction reference electrodes. The electric potential difference across the reference electrodes, E_x was recorded using a multimeter (Model 2000, Keithley, Cleveland, OH) as a function of time using a LabView program. Typically, the electric potential stabilized after 20 to 30 minutes (cf. figure 2). The potential, E_x was recorded every 10 seconds, and the stabilized condition was defined as the point where the rate of change in E_x was less than 0.3 mV over 20 minutes. The value of E_x was taken as a time average of the electric potential difference measurements made over 30 minutes following stabilization of the potential.

The offset potential of the reference electrodes, E_{offset}, was measured after completion of the E_x measurement. This offset potential captured the asymmetry of the specific reference electrodes that were used in the measurement. Both reference electrodes were placed in the high concentration solution, and the electric potential difference between the reference electrodes was measured using a multimeter. The value of E_{offset} was determined by averaging the offset potential over a period of 30 minutes to 1 hour once the offset potential had stabilized. Equation X was used to determine the membrane potential.

Solution concentrations were chosen to be $C_0 = 0.1$ mol/L and C_L = 0.5 mol/L for measurements with commercial membranes and $C_0 = 0.1$ mol/L and C_L = 0.2 mol/L for lab-prepared XLAMPS. These concentrations should ensure that the electric potential, E_x, would be sufficiently large to measure accurately. The average electrolyte activity values were determined as:

$$a_{\pm}^{s0} = \gamma_{\pm}^{s0} C_0 \tag{7}$$

$$a_{\pm}^{sL} = \gamma_{\pm}^{sL} C_L \tag{8}$$

where $\gamma_{\pm}^{s0}$ and $\gamma_{\pm}^{sL}$ are the average electrolyte activity coefficients on the low and concentration sides of the membrane, respectively, and these activity coefficients were calculated using the Pitzer model.[41] The counter-ion and co-ion transport numbers in solution were calculated from equation 9:

$$t_i^s = \frac{|z_i| C_i^s D_i^s}{\sum_j |z_j| C_j^s D_j^s} \tag{9}$$

where z_i is the ion charge, c_i^s is the concentration of ion in solution, and D_i^s is the self-diffusion coefficient of ion i. Since only sodium chloride (a monovalent, strong electrolyte) was used in this study, the counter-ion concentration in solution was taken to be equal to the co-ion concentration in solution.

2.2.3.1 Temperature Dependence of Apparent Permselectivity

To probe the influence of temperature on apparent permselectivity, fresh solution baths (Figure 1) were cooled or heated using a water bath. To prevent evaporation, the solution baths were connected to the measurements such as the solution was not exposed to the atmosphere until it exited the tubing after passing through the measurement cell. A probe was placed in the low concentration solution chamber to measure the temperature, and the water bath temperature was set such that the desired chamber temperature was achieved. Chamber temperatures were set in the range of 14^{o}C to 31^{o}C. These temperatures were selected to be both above and below typical room temperature to determine whether modest temperature fluctuations appreciably influence the apparent membrane permselectivity measurement.

2.2.3.2 Flow Rate Dependence of Apparent Permselectivity

Apparent permselectivity was measured using a series of single pass solution flow rates, ranging from 1 to 15 mL/min, to determine the minimum flow rate that would maintain the solution concentration in both chambers of the experimental apparatus (i.e., maintain the pseudo-steady state condition during the measurement). Flow rates were controlled using a digital peristaltic pump (Masterflex L/S Digital Drive, Cole-Parmer, USA). Fresh solution was fed to the chambers, and the displaced solution was not recycled to the chambers.

2.2.4 Error Propagation Analysis

Uncertainty resulting from the electric potential measurements and the solution preparation process was taken into consideration using standard error propagation analysis.[42] The magnitude of electric potential measurement fluctuations, ΔE, an independent variable for the purpose of this error propagation analysis, was taken to be a series of values ranging from 0 to 0.4 mV, which was found to be an experimentally relevant range. The uncertainty of the membrane apparent permselectivity, $\Delta\alpha$, was calculated using ΔE and standard error propagation techniques. The deviations from the target solution concentrations for low concentration, ΔC_0, and high concentration, ΔC_L, solutions, independent variables for the purpose of this error propagation analysis, were taken to be a series of values ranging from 0 to 0.015 mol/L and 0 to 0.075 mol/L, respectively, and values of $\Delta\alpha$ were calculated using ΔC_0 or ΔC_L and standard error propagation techniques. The effect of error in the salt mass measurement, Δm, associated with the preparation of 1 L of low and high concentration solution on the membrane permselectivity was also investigated. Values of Δm ranging from 0 to 100 mg (NaCl) were considered, and standard error propagation techniques were used to determine the influence of Δm on the uncertainty of the apparent permselectivity.

2.2.5 Kinetic Desorption

Kinetic desorption measurements were conducted on lab-prepared membranes to obtain membrane salt sorption and diffusion coefficient.[38, 43] When the membrane sample thickness is controlled to be much smaller than the diameter, the diffusion of salt out of the sample could be approximated as a one dimensional unsteady-state diffusion process and desorption concentration at each time point could be obtained by solving a partial differential equation. By tracking the desorption concentration at each different time points and at infinite time, the membrane salt sorption coefficient and diffusion coefficient could be obtained.[44] In this study, the membrane samples were cut into circular sample coupons with diameter ranging from 0.95

cm to 2.22 cm, whereas the membrane thickness were controlled to be around 250 µm such that the one dimensional unsteady-state diffusion assumptions applied.

Prior to measurements, the circular membrane sample coupons were soaked in salt solutions with considered concentrations (i.e., 0.1 mol/L or 0.2 mol/L) for 24 to 36 hours. This soaking time should allow the membrane to be fully equilibrated with external solutions.[37] During the measurements, the membrane sample was taken out of the salt solution and the excess solution on the sample surface was carefully wiped off by a laboratory tissue. Then the sample was immediately transferred into a beaker containing 25mL to 150mL DI water, depending on the estimated amount of salt in the sample and the target desorption concentration (typically 2 to 5 ppm). The solution was stirred by a stirring bar or an overhead stirrer and the conductivity of the desorption solution was recorded every 10 to 60 seconds using a conductivity benchtop meter (inoLab® Cond7310, WTW Corp Inc., CA, USA). The desorption process was stopped when the conductivity of the desorption solution was observed to remain constant for a time period that is longer than half of the total desorption time. After the desorption process, the desorption solution concentration was then calculated using a calibration curve which was made before the desorption measurements. The solution concentration at each time point was recorded as C_t^s, and the solution concentration at infinite time was recorded as C_∞^s. Then $\frac{C_t^s}{C_\infty^s}$ was plotted as a function of the square root of time $\sqrt{\mathrm{t}}$, as shown in Figure 5. At small time and small desorption concentration ($\frac{C_t^s}{C_\infty^s} < 0.6$), the corresponding relationship between c_t^s and c_∞^s can be approximated as:

$$\frac{C_t^s}{C_\infty^s} \cong \left(\frac{16 D_s^m}{\pi \delta^2} t\right)^{\frac{1}{2}} \tag{9}$$

where: D_s^m is the salt diffusion coefficient, δ is the hydrated membrane thickness.

The hydrated sample thickness δ, as then immediately measured using a micrometer (Model No. 293-344, Mitutoyo, U.S.A). Thickness was measured at 3 to 5 different places of the sample and the final reported value was the average of 3 to 5 measurements. The hydrated membrane diameter d, was also measured using a laboratory ruler. After that, the salt diffusion coefficient D_s^m, could be calculated from measured membrane thickness and slope of the linearly fitted initial desorption curve, as shown in Figure 5.

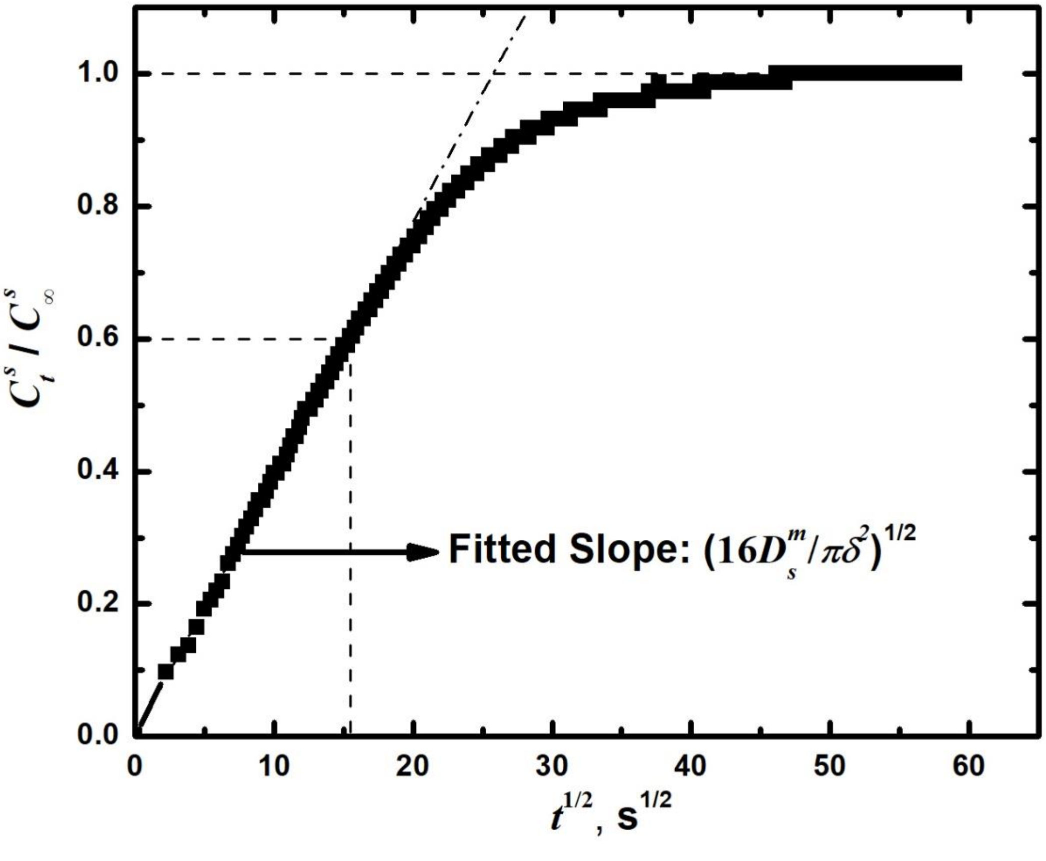

Figure 5. Schematic illustration of data analysis for desorption measurement

The membrane salt sorption coefficient K_s, could be calculated from membrane salt concentration C_s^m and external salt concentration, C_s^s, where the membrane concentration was could be obtained from c_∞^s, desorption volume V_d, and hydrated sample volume V_p, as shown in equation 10:

$$K_s = \frac{c_s^m}{c_s^s} = \frac{c_\infty^s V_d}{c_s^s V_p} \tag{10}$$

Since the membrane in this study were all cut into circular samples, the hydrated membrane volume was calculated as:

$$V_p = \frac{\pi \delta d^2}{4} \tag{11}$$

3. Results and Discussion

3.1 The Effect of Experimental Factors on Apparent Permselectivity

3.1.1 Temperature and Flow Rate

Temperature variations around room temperature could affect apparent permselectivity, and little is known about the temperature sensitivity of this property. The membrane apparent permselectivity decreases slightly as temperature increases (Figure 6). These effects are relatively small as increasing temperature from 14°C to 31°C results in a decrease in apparent permselectivity that is less than 2% for both commercial membranes. Therefore, under typical experimental conditions (i.e., room temperature with fluctuations that do not exceed ±5°C), some temperature-induced apparent permselectivity fluctuations may occur, but these fluctuations should be relatively small (no larger than 2%). The standard deviation from the mean of the three replicate values (i.e., the error bars in Figure 6) is generally in the range of 1% to 2% for these measurements, so the dependence of apparent permselectivity on temperature, over this temperature range, is on the order of the uncertainty that results from simply dismantling the cell and reassembling the cell to conduct replicate measurements

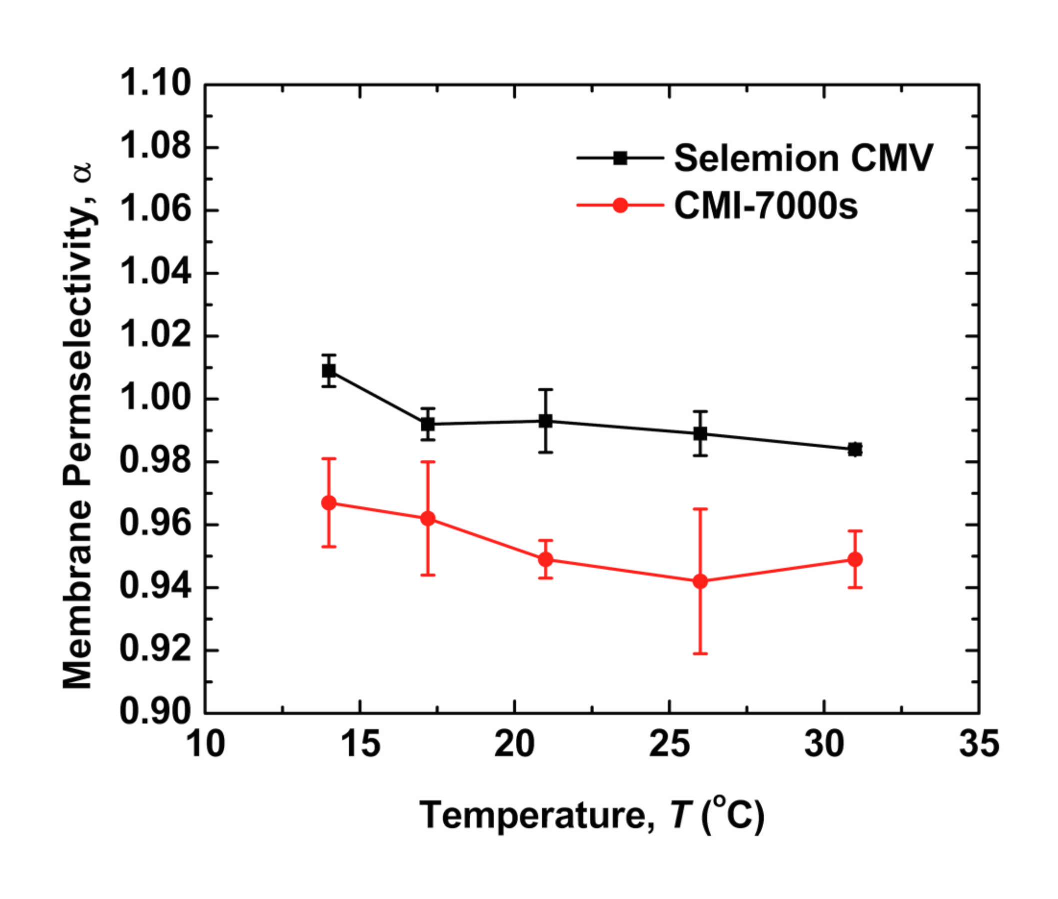

Figure 6. Apparent permselectivity decreases slightly as temperature increases over a modest range of temperatures surrounding room temperature. The apparent permselectivity was characterized using 0.1 mol/L and 0.5 mol/L aqueous sodium chloride solutions. Fresh solution single-pass flow rates were 5 mL/min. Each data point corresponds to the average of three replicate measurements made on a membrane sample (the cell was disassembled and reassembled between measurements), and the error bars correspond to one standard deviation from this average.

The rate of fresh solution addition to each chamber will influence the solution residence time in the chamber, and this residence time influences the formation of the pseudo-steady state measurement condition. During the measurement, the solution concentration on both sides of the membrane should be effectively constant, and achieving this pseudo-steady state condition requires a sufficiently high flow rate of fresh solution to be provided to each chamber. In order to maintain the concentration on both sides of the membrane, the solution residence time, τ, must be much shorter than the diffusion time scale, t_{diff}, for salt permeation through the membrane. Thus, $\frac{\tau}{t_{diff}} = \frac{V_c/f}{\delta^2/D_s} \ll 1$ where V_c is the volume of the chamber, f is the solution flow rate, δ is the membrane thickness, and D_s is the salt diffusion coefficient in the membrane.

Apparent permselectivity values were measured using a series of flow rates (1 to 15 mL/min). Above 5 mL/min, the apparent permselectivity stabilizes for both membranes (Figure 7), suggesting that those flow rates are sufficient to achieve the pseudo-steady state condition. The sensitivity of apparent permselectivity to flow rate is more pronounced for the Selemion CMV membrane, and the CMI membrane achieves the pseudo-steady state condition at a flow rate of 3mL/min, which is lower than that required for the CMV membrane. This situation could be explained by the time scale relationship described above. The CMV membranes are thinner than the CMI membranes (Table 1), so the diffusion time scale of the CMV membrane is much shorter than that of the CMI membrane. Thus, a greater flow rate must be used with the CMV membrane to reduce the solution residence time compared to what is required for the CMI membrane. This analysis also explains why the CMI membrane is less sensitive to flow rate than CMV membrane. Thicker membranes, such as the CMI membrane, have larger diffusion time scales, so the pseudo-steady state condition can be achieved at lower flow rates.

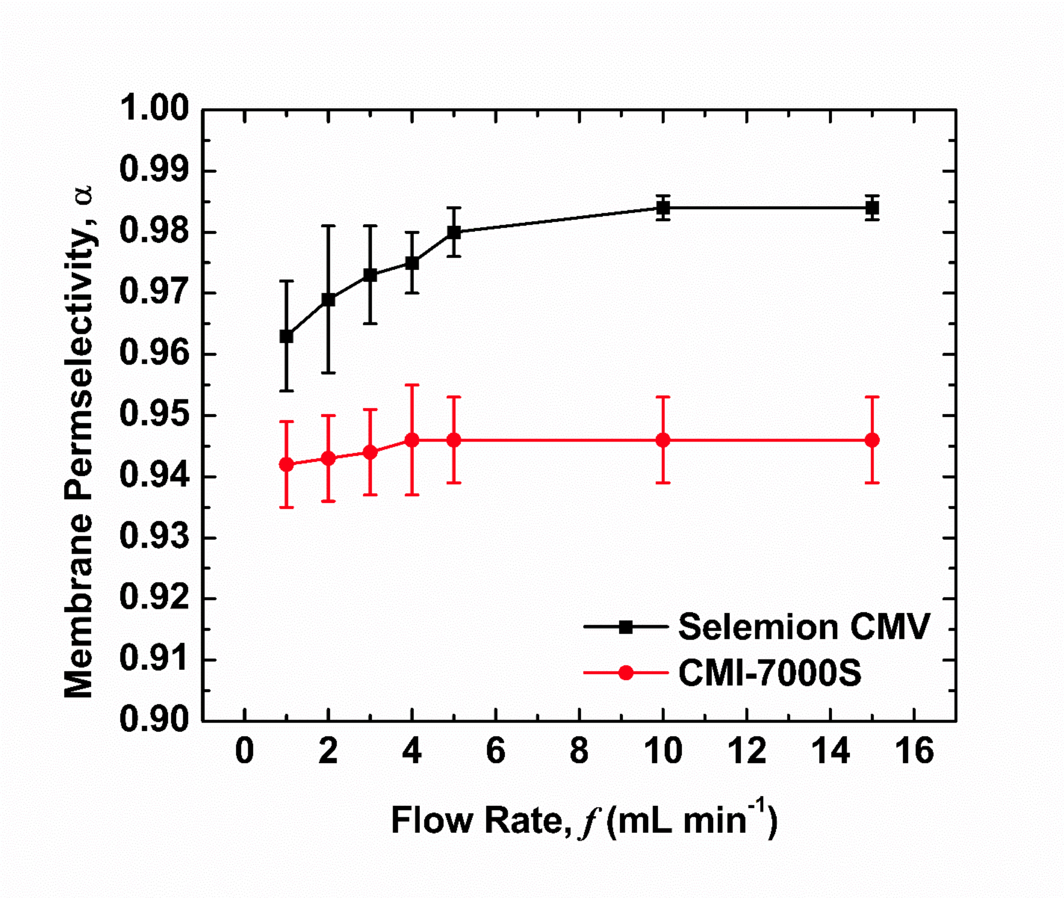

Figure 7. Apparent permselectivity as a function of solution flow rate at 21°C. The apparent permselectivity was characterized using 0.1 mol/L and 0.5 mol/L aqueous sodium chloride solutions. Each data point corresponds to the average of three replicate measurements made on a membrane sample (the cell was disassembled and reassembled between measurements), and the error bars correspond to one standard deviation from this average.

3.1.2 Concentration Deviation

The relationship between concentration deviations and apparent permselectivity for low concentration solution and high concentration solution are shown in Figure 8a and 8b. Figure 8a shows the situation for deviations around a C_L = 0.5 mol/L NaCl solution, and Figure 8b shows the situation for deviations around a C_0 = 0.5 mol/L NaCl solution. The actual solution concentration is normalized by the target concentration (i.e., 0.1 mol/L or 0.5 mol/L), and the actual apparent permselectivity is also normalized by the value measured using the target solution concentrations.

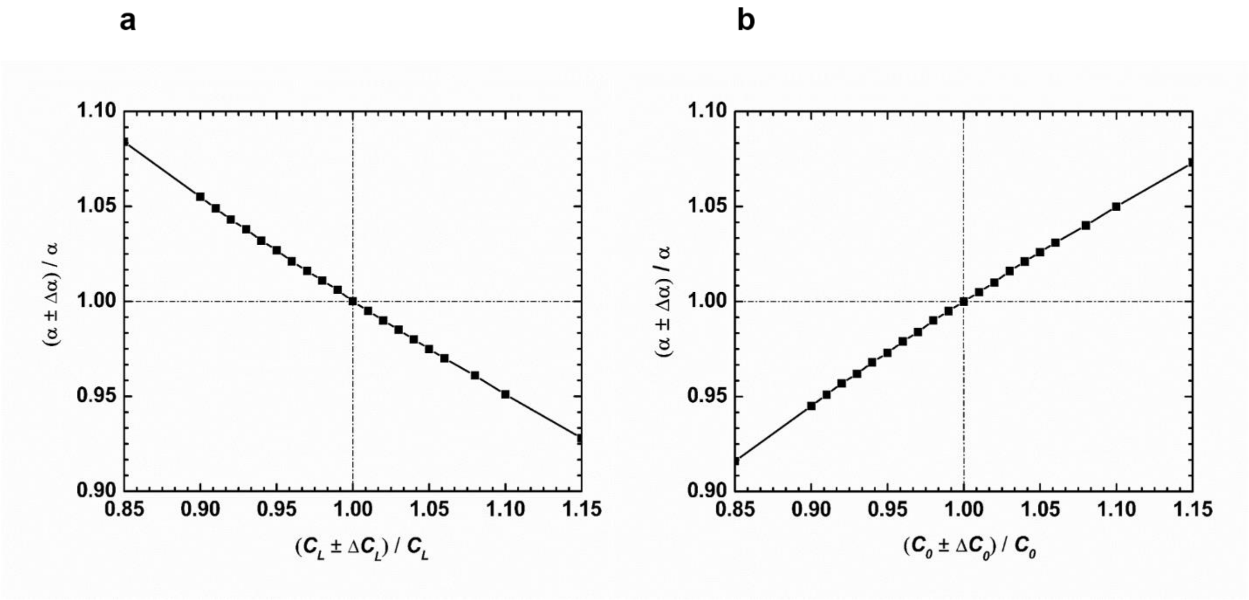

Figure 8. Error analysis reveals the relative deviation of the apparent permselectivity as a function of the relative deviation of solution concentration for: (a) the high concentration solution and (b) the low concentration solution.

The influence of concentration changes on apparent permselectivity depends whether the change increases or decreases the difference of the thermodynamic activity values of the solutions on either side of the membrane. When the value of C_L increases (i.e., $\Delta C_L > 0$) with a fixed value of C_0, the difference of thermodynamic activity values of the solutions on either side of the membrane increases. This situation results in an increase in the apparent permselectivity (Figure 8a) compared to the base case ($C_L = 0.5$ mol/L). For example, if the concentration of the high concentration solution was 5% greater than the base case (i.e., $\Delta C_L = 0.025$ mol/L), the measured apparent permselectivity would increase by approximately 2.8% compared to the base case. When the value of C_0 increases (i.e., $\Delta C_0 > 0$) with a fixed value of C_L, the difference of thermodynamic activity values of the solutions on either side of the membrane decreases. This situation results in an decrease in the apparent permselectivity (Figure 8b) compared to the base case ($C_0 = 0.1$ mol/L). For example, if the concentration of the high concentration solution was

5% greater than the base case (i.e., ΔC_0 = 0.005 mol/L), the measured apparent permselectivity would decrease by approximately 2.8% compared to the base case. Therefore, concentration changes that increase the activity difference across the membrane cause an increase in apparent permselectivity and vice versa.

Uncertainty in the measurement of salt mass, while preparing the salt solutions, is one possible source of error in the salt solution concentrations. While the relationship between the relative magnitudes of concentration and apparent permselectivity uncertainty is similar for the high and low concentration solutions (as discussed in the preceding paragraph and Figure 8), the influence of absolute magnitude of uncertainty in the solution preparation process (e.g., uncertainty in the mass of salt measured during the solution preparation process) has a more significant effect on apparent permselectivity if the uncertainty is in the low concentration solution compared to the high concentration solution (Figure 9). For example, preparation of 1 L of 0.1 mol/L and 0.5 mol/L aqueous NaCl solution requires measuring 5.844 g and 29.22 g of sodium chloride, respectively. A 10 mg salt mass deviation in the 0.1 mol/L solution will introduce a 0.1% deviation in apparent permselectivity. The same mass deviation in the 0.5 mol/L solution will only introduce a 0.015% deviation in apparent permselectivity. Therefore uncertainty in the salt mass measured during the solution preparation process will influence the low concentration solution to a greater extent than the high concentration solution.

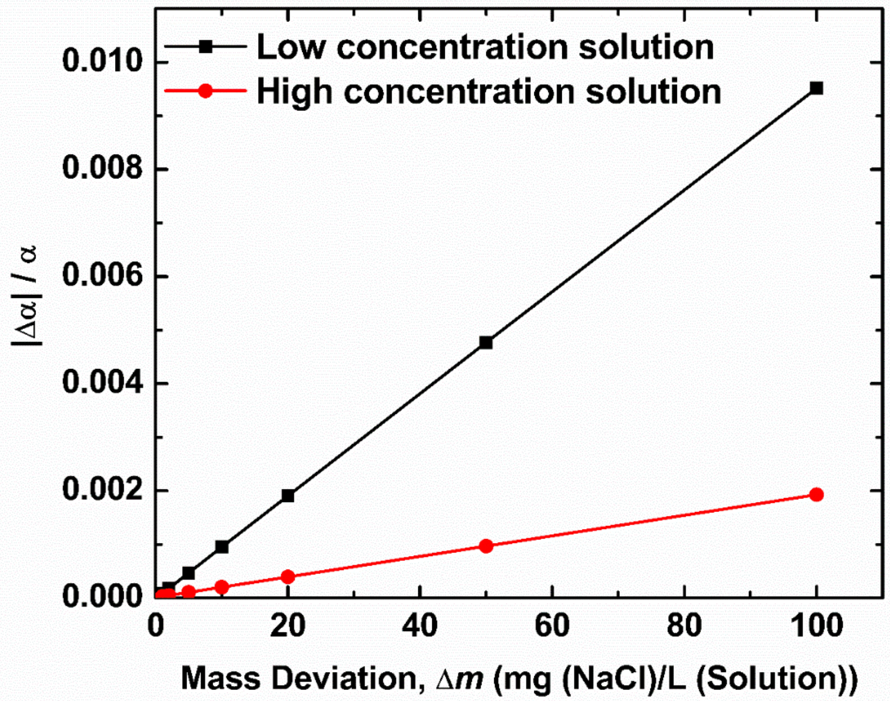

Figure 9. Uncertainty in the salt mass measured during the solution preparation process, Δm, has a more significant influence on apparent permselectivity if the uncertainty is in the low concentration solution compared to the high concentration solution.

In addition to potential salt mass measurement errors, which could contribute to Δm, sorption of atmospheric moisture into the salt crystals and/or losses during solute transfer (after the mass measurement) could also contribute to Δm and thus affect the apparent permselectivity. These contributions, however, may be small in practice. Deviations from target sodium chloride solution concentrations of 10 ppm in the high and low concentration solutions introduces approximately 0.015% and 0.1% error, respectively, in apparent permselectivity, and this uncertainty is within the replicate uncertainty that results from disassembling and reassembling the measurement cell between replicate apparent permselectivity measurements.

3.1.3 Electric Potential

During the apparent permselectivity measurement, the measured value of E_x increased and reached a stabilized value (cf. Figure 2). The final measured value of E_x was taken as the average electric potential, and the standard deviation ΔE was taken as the measurement uncertainty. The membrane potential, E_m, was determined using the measured electrode offset potential (Equation 4). The uncertainty in the measurement of E_{offset} was typically more than 2 orders of magnitude smaller than the value of ΔE, so the value of ΔE was taken as the uncertainty in E_m. A ΔE value that is 1% of E_m will introduce approximately a 1% deviation in the final membrane apparent permselectivity (Figure 10). For the conditions (0.1 mol/L and 0.5 mol/L NaCl solutions) used in this study, average membrane potential values, E_m, were around 37 mV, and in this case, typical values of ΔE ranged from 0.1 mV to 0.2 mV. Therefore, fluctuations in the measurement of E_m contribute roughly 0.2% to 0.5% uncertainty in the final apparent permselectivity. In contrast, the concentration variability of low concentration solution and high concentration solution typically introduce about 0.015% to 0.1% uncertainty in the final apparent permselectivity, and the uncertainty from temperature fluctuations is expected to be no larger than 2%.

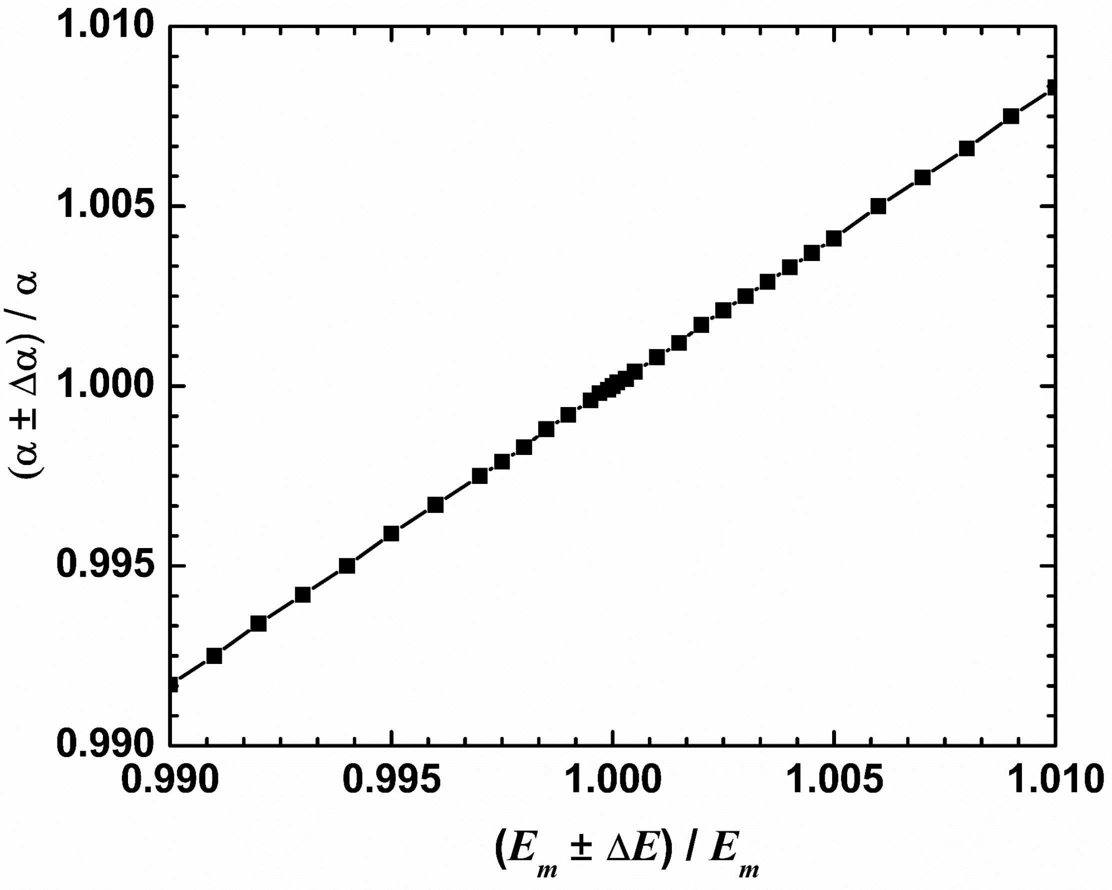

Figure 10. Fluctuations in the membrane potential measurement (ΔE) introduce uncertainty in the apparent permselectivity.

3.2 The Effect of Co-ion Identities on Membrane Permselectivity

Permselectivity of XLAMPS was measured with four different monovalent salts, sodium chloride, sodium bromide, sodium nitrate and sodium perchlorate, with concentration of 0.1 mol/L and 0.2 mol/L. When different co-ions were used, the permselectivity of XLAMPS was demonstrated to be different, and followed the trend: $\alpha_{\mathrm{NaCl}} > \alpha_{\mathrm{NaNO_3}} > \alpha_{\mathrm{NaBr}} > \alpha_{\mathrm{NaClO_4}}$, as presented in Figure 11a. The normalized salt sorption and diffusion coefficients of XLAMPS were also presented in Figure 11b to demonstrate a competing mechanism between salt sorption coefficient and salt diffusion coefficient in determining the relative magnitude of permselectivity among these four salts. The sorption coefficients and diffusion coefficients were all normalized by the values of sodium bromide, therefore sodium bromide would serve as a reference in the following discussion.

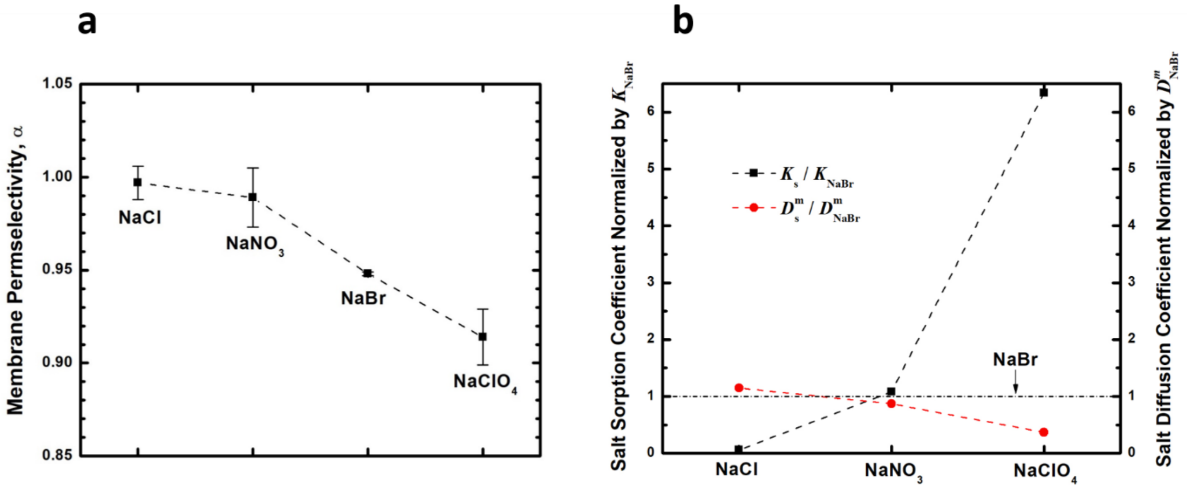

Figure 11. (a) Permselectivity of XLAMPS measured using four monovalent salts, with concentration range of 0.1 mol/L and 0.2 mol/L (b) Salt sorption coefficients and diffusion coefficients of XLAMPS, normalized by the values of sodium bromide. Salt sorption coefficients were measured using 0.2 mol/L external solutions, salt diffusion coefficients were measured using samples equilibrated in 0.2 mol/L salt solutions.

As demonstrated previously, permselectivity is inversely correlated with either co-ion sorption or co-ion diffusion, i.e., higher amount of co-ion sorption with fixed co-ion diffusion coefficient or higher co-ion diffusion coefficient with fixed amount of co-ion sorption will result in lower permselectivity. For the four salts considered in this study, their sorption coefficients represent for the co-sorption effects and follow the trend: $K_{\mathrm{NaClO_4}} > K_{\mathrm{NaNO_3}} > K_{\mathrm{NaBr}} > K_{\mathrm{NaCl}}$. Their diffusion coefficients represent for the co-ion diffusion effects follow opposite trends, in that: $D^m_{\mathrm{NaCl}} > D^m_{\mathrm{NaBr}} > D^m_{\mathrm{NaNO_3}} > D^m_{\mathrm{NaClO_4}}$. The relative magnitude of permselectivity between two salts is determined by either their difference in sorption coefficients or diffusion coefficients, whichever is larger. For example, K_{NaCl} is 0.41 times lower than K_{NaBr}, whereas D^m_{NaCl} is only 0.15 times higher than D^m_{NaBr}. The difference between their sorption coefficients is larger than the difference between their diffusion coefficients, hence sorption effects dominates in determining their relative magnitude of permselectivity. In that case, $K_{\mathrm{NaBr}} > K_{\mathrm{NaCl}}$ will lead to $\alpha_{\mathrm{NaCl}} > \alpha_{\mathrm{NaBr}}$. On the other hand, $K_{\mathrm{NaNO_3}}$ is about 0.08 times higher than K_{NaBr}, whereas $D^m_{\mathrm{NaNO_3}}$ is about 0.14 times lower than D^m_{NaBr}. In this case, diffusion effects dominates in determining their relative magnitude of permselectivity and $D^m_{\mathrm{NaBr}} > D^m_{\mathrm{NaNO_3}}$ will lead to $\alpha_{\mathrm{NaNO_3}} > \alpha_{\mathrm{NaBr}}$. The situation becomes even clearer with sodium perchlorate since its sorption coefficient is much higher than the sorption coefficient of sodium bromide. For sodium bromide, $K_{\mathrm{NaClO_4}}$ is about 5.3 times larger than K_{NaBr}, whereas $D^m_{\mathrm{NaClO_4}}$ about 1.7 times lower than D^m_{NaBr}. Sorption effects absolutely dominates and $K_{\mathrm{NaClO_4}} > K_{\mathrm{NaBr}}$ will lead to $\alpha_{\mathrm{NaBr}} > \alpha_{\mathrm{NaClO_4}}$.

This competing mechanism, again revealed that permselectivity is a combined result of co-ion sorption and co-ion diffusion. Therefore, the effects of any co-ion specific factors on membrane permselectivity, are fundamentally attributed to their effects on co-ion sorption or co-ion diffusion. The absolute value of the sorption coefficients and diffusion coefficients of these salts, are then of great interest.

3.3 Salt (Co-ion) Sorption

The salt sorption coefficients of XLAMPS were measured with sodium chloride, sodium bromide, sodium nitrate and sodium perchlorate to investigate their contributions to membrane permselectivity. The membrane salt sorption coefficients were measured with 0.1 mol/L and 0.2 mol/L salt solutions, as presented in Figure 12. Since the cations was fixed as sodium, the difference among salt sorption coefficients should reflect different co-ion sorption behaviors.

Traditionally, the co-ion exclusion behavior of charged, highly-swollen polymeric membranes were quantitatively predicted by Donnan exclusion.[1, 9, 45, 46] According to Donnan exclusion, the salt (co-ion) sorption coefficient for monovalent salts in charged membrane is a function of membrane fixed charge group concentration C_A^m, and external salt concentration C_s^s:[9, 45]

$$K_s \equiv \frac{C_s^m}{C_s^s} = \left[\frac{1}{4}\left(\frac{C_A^m}{C_s^s}\right)^2 + 1\right]^{\frac{1}{2}} - \frac{1}{2}\frac{C_A^m}{C_s^s} \qquad (10)$$

It is predicted by Donnan exclusion that the salt sorption coefficient K_s increases with increasing external salt solution and decreases with increasing fixed charge group concentration.[37] The experimental results are consistent with Donnan exclusion in the way that as external salt concentration increases from 0.1 mol/L to 0.2 mol/L, the sorption coefficient K_s of all salts increase as well. However, since salt valence are the only adjustable parameters in equation 10, it fails to predict the different sorption coefficients of these four monovalent salts with XLAMPS, as presented in Figure 11. The experimentally measured salt sorption coefficients K_s show the trend: $K_{\mathrm{NaClO_4}} > K_{\mathrm{NaNO_3}} > K_{\mathrm{NaBr}} > K_{\mathrm{NaCl}}$, whereas the predicted salt sorption coefficients by Donnan exclusion stay uniform for the four salts.

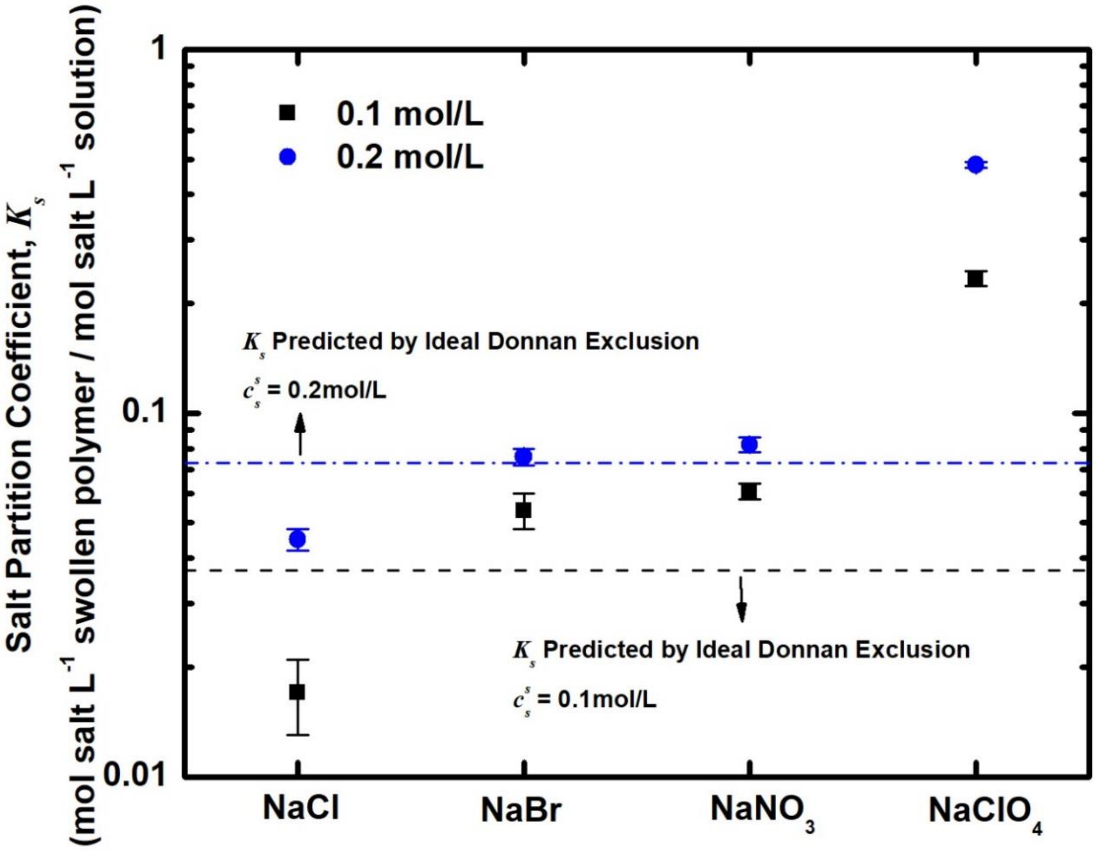

Figure 12. Salt sorption coefficient K_s of XLAMPS membrane, measured with 0.1 mol/L and 0.2 mol/L salt solutions. The external concentration values correspond to the concentration range used for the membrane permselectivity measurements.

Note that equation 10 is a simplified version of Donnan exclusion, where the membrane activity coefficient is assumed to be equal to solution activity coefficient, i.e., activities are approximated to be equal to concentrations.[9] It is somewhat challenging to take the effect of activity coefficients into considerations since an widely-applicable, widely-recognized model predicting the ion activity coefficient in charged polymer is not yet available. Recently, Manning’s counter-ion condensation theory has been combined with Debye-Huckel theory and Pitzer’ model by Kamcev et al. to predict the ion activity coefficient in charged polymeric membrane.[46] This model is an applicable approach to estimate activity coefficients in charged membrane. But since it requires experimentally measured membrane concentration as an input, its final prediction of sorption coefficient is not absolutely independent of experimental values, so its applicability is still doubtful. The prediction from Kamcev's model will not be presented in this study for the sake of saving space, but more future efforts needs to be conducted to include ion activity coefficients into equation 10.

A continuum model was applied in this study to investigate the role of bare ion size and excess polarizability in ion sorption by predicting the free energy change associated with moving an ion from solution phase into membrane phase based on the bare ion radius and excess ion polarizability.[47-49] This model was proposed by Ninham et al.[48] According to this model, the total energy associated with moving an ion from external solution phase into membrane phase is the sum of electrostatic solvation energy and dispersion energy. The electrostatic energy part is calculated from Born's model,[28, 50, 51] which accounts for the electrostatic solvation energy change of moving ion from solution phase into membrane phase by assuming the ion is non-polarizable.[31] The dispersion part is developed by Ninham et al., which accounts for the extra electrodynamic dispersion energy change of moving ion from solution into membrane when the ion is polarizable and its polarizability is different from the surrounding medium.[47] The total free energy is then calculated as:

$$\Delta G^{Total} = \Delta G^{Ele} + \Delta G^{Disp} = \frac{z_i^2 e^2}{8\pi\varepsilon_0 a_i}\left(\frac{1}{\varepsilon_m(0)} - \frac{1}{\varepsilon_{sol}(0)}\right) + \frac{4k_B T}{a_i^3\sqrt{\pi}}\sum_{n=0}^{\infty}\left[\frac{\alpha_m^*(i\omega_n)}{\varepsilon_m(i\omega_n)} - \frac{\alpha_{sol}^*(i\omega_n)}{\varepsilon_{sol}(i\omega_n)}\right] \qquad (11)$$

where: z_i is the valence of the ion; e is the elementary charge, ε_0 is the permittivity of free space; k_B is Boltzmann's constant; T is temperature, ; $\varepsilon_m(0)$ is the membrane relative permittivity under zero frequency, which was often referred as dielectric constant in some previous literature and was taken as the value for hydrocarbon thin film (taken to be 2 in this study[52]); $\varepsilon_{sol}(0)$ is the relative permittivity of external solution under zero frequency (taken to be 80 for aqueous electrolytes[53]); a_i is the bare ion cavity radius;[54] $\alpha_m^*(i\omega_n)$ and $\alpha_{sol}^*(i\omega_n)$ are the excess ionic polarizability as a function of considered frequencies in membrane phase and solution phase, whereas the excess ionic polarizability in water were all used in this study;[28] $\varepsilon_m(i\omega_n)$ is the relative permittivity of membrane, $\varepsilon_{sol}(i\omega_n)$ is taken as the relative permittivity of water, and is obtained from experimental data.[55] ω_n is a series of discrete frequencies under consideration. $\omega_n = k_B T n/h \; (n = 0,1,2 \ldots)$ where $n = 0$ term means it starts from $\frac{1}{2}$, and h is the Planck constant.

The excess ion polarizability in water, was modeled using a sing oscillator model:[48, 52]

$$\alpha_m^*(i\omega_n) = \alpha_{sol}^*(i\omega_n) = \frac{\alpha^*}{1+\omega_n^2/\omega_I^2} \tag{12}$$

where: α^* is the ionic excess polarizability at zero frequency in water;[54] ω_I is the sing adsorption frequency of a single ion and was typically calculated from first ionization potential;[27]

The relative permittivity of membrane as a function of frequency, was also modeled with a single oscillator frequency:[48, 52]

$$\varepsilon_m(i\omega_n) = 1 + \frac{\varepsilon_m(0)-1}{1+\omega_n^2/\omega_{uv}^2} \tag{13}$$

where: $\varepsilon_m(0)$ is the membrane relative permittivity at zero frequency, and was taken to be 2 as mentioned above; ω_{uv} is a characteristic frequency of the membrane and was taken to be 10^{16} rad/s for hydrocarbon film. [46]

All the ionic properties used in this calculation were also shown in table 3:

Table 3. Anion properties used in energy calculation

Ions	$\mathbf{Cl^-}$	$\mathbf{Br^-}$	$\mathbf{NO_3^-}$	$\mathbf{ClO_4^-}$
$\boldsymbol{\alpha^*}$ **($\boldsymbol{\AA^3}$)**	4.7	6.1	7.0	8.3
$\boldsymbol{\omega_I}$ **($\mathbf{10^{16}}$ rad/s)**	1.97	1.8	2.13	2.56
$\boldsymbol{a_i}$ **($\boldsymbol{\AA}$)**	1.81	1.96	1.79	2.20

The dispersion energy part then ends up being a summation over discrete frequencies ($\omega_n = k_B T n/h$), but the first several hundred terms constitutes the largest part. In this study, only the first 150 terms were considered due to the lack of water relative permittivity data. This might underestimate the dispersion energy slightly but should not harm the general results and principles. Under all the conditions and assumptions above, the total free energy of transferring the ion from solution phase into membrane phase were calculated and results were reported in Figure 12.

The electrostatic free energy part, dispersion energy part were then calculated and added up. The calculated total free energy was then compared with the experimentally measured total free energy ΔG^{Exp}, as related with experimentally measured sorption coefficient:[31]

$$K_s \equiv \frac{C_s^m}{C_s^s} = \exp\left[-\frac{\Delta G^{Exp}}{RT}\right] \tag{14}$$

Note that 14 is also based on the assumption of solution ideality since the activity coefficients have been set equal to unity.

The comparison among electrostatic free energy, total free energy, and experimental free energy is presented in Figure 13, where the sorption coefficients required for calculating experimental free energy though equation 14 were measured using XLPEGDA (n=3) membrane with 0.1 mol/L salt solutions. The reason for such choice of experimental data will be explained later. The salt sorption coefficient of XLPEGDA (n=3) follows the trend: $1 > K_{\mathrm{NaClO_4}} >$

$K_{\mathrm{NaNO_3}} > K_{\mathrm{NaBr}} > K_{\mathrm{NaCl}}$. The experimental free energy change is then calculated and demonstrated to be energy barrier (i.e., $K_s < 1$ and $\Delta G^{Exp} > 0$) and follows the trend: $\Delta G^{Exp}_{NaCl} > \Delta G^{Exp}_{NaBr} > \Delta G^{Exp}_{\mathrm{NaNO_3}} > \Delta G^{Exp}_{\mathrm{NaClO_4}}$.

The electrostatic free energy was calculated by Born's model, (i.e., the first part on the right hand side of equation 11) in which the ionic charge and bare ion radius are the only ion specific parameters that influence the energy change. When only electrostatic energy is considered, the estimated total free energy change is substantially higher than experimental values, showing that the Born's model might overestimate total energy barrier. In addition, the total free energy change calculated by Born's model follows the trend: $\Delta G^{Ele}_{\mathrm{NaNO_3}} > \Delta G^{Ele}_{NaCl} > \Delta G^{Ele}_{NaBr} > \Delta G^{Ele}_{\mathrm{NaClO_4}}$, indicating that smaller bare ion radius results in higher electrostatic energy barrier. However, the prediction by Born's model shows inconsistency with experimental values in that $\Delta G^{Ele}_{\mathrm{NaNO_3}}$ is larger than ΔG^{Ele}_{NaCl} and ΔG^{Ele}_{NaBr}, which points out that bare ion radius is probably not the only contributing parameter. Other effects must be considered as well to obtain at least a qualitative agreement between prediction and experiment.

The dispersion free energy was then calculated by Ninham's model, (i.e., the second part on the right hand side of equation 11) where the ion excess polarizability α^* and bare ion radius a_i were supposed to affect free energy change in the form of $\frac{\alpha^*}{a_i^3}$. Dispersion free energy was calculated to be negative, indicating that it facilitates ion transferring from solution phase to membrane phase, so the gap between estimated total energy and experimental total energy was narrowed after the dispersion energy was incorporated. It can also be revealed from Figure 13 that the modified total free energy (with dispersion energy included) exhibits better qualitative consistency with the experimental total free energy. The incorporation of dispersion energy compensated the high electrostatic energy barrier for sodium nitrate, thus leading the calculated total free energy to show the same trend with the experimental free energy, i.e., $\Delta G_{NaCl}^{Total} > \Delta G_{NaBr}^{Total} > \Delta G_{\mathrm{NaNO_3}}^{Total} > \Delta G_{\mathrm{NaClO_4}}^{Total}$.

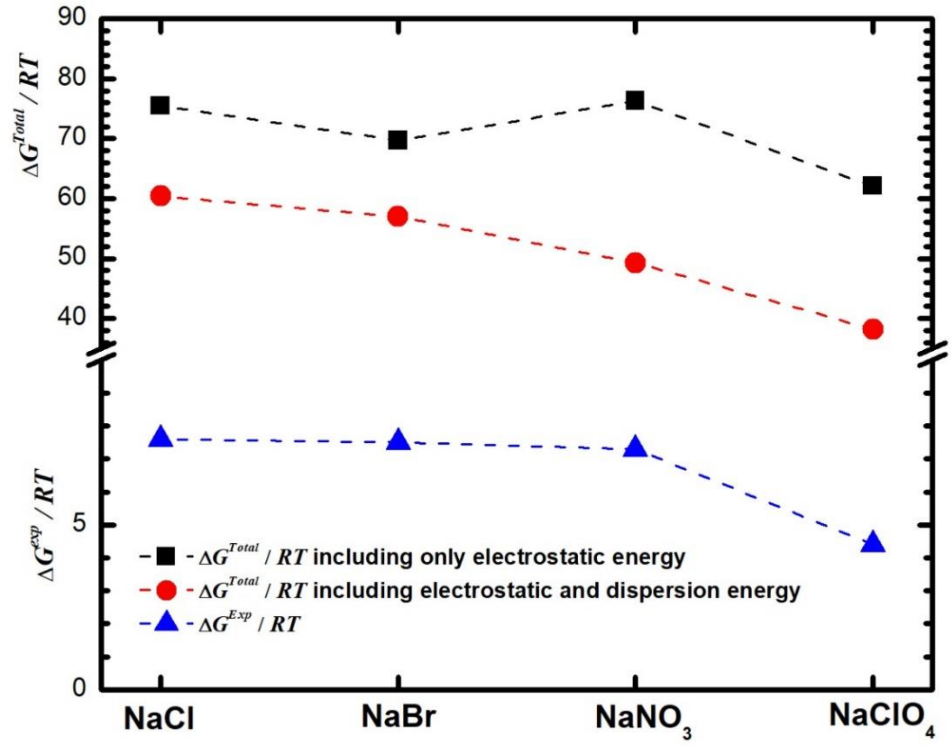

Figure 13. The comparisons among estimated total free energy with only electrostatic part, estimated total free energy with both electrostatic and dispersion part, and experimentally obtained total free energy from equation 14. The experimental sorption coefficients data were measured using XLPEGDA (n=3), with four salt solutions of 0.1 mol/L. The reason for such choice of membrane material will be discussed later.

So far, all of the calculations discussed above are rough estimations. There are still a lot of debates in this area with regard to the validity of the continuum dielectric assumption[47] and the proper choice of ion and polymer related parameter (e.g. whether the covalent radius or the ionic radius should be used).[54] Whereas the qualitative consistency between estimated total free energy change and experimental total free energy change at least demonstrates that the ion excess polarizability, as well as ion size, plays a role in explaining the co-ion specific phenomena in co-ion sorption, and both of them need to be evaluated more systematically in the future.

3.4 Effects of $NaClO_4$-ethylene oxide Complexation on Salt (Co-ion) Sorption

Back to figure 12, although Donnan exclusion prediction fails to differentiate the four salts, it seems to at least provide a reasonable estimation for sorption coefficients associated with sodium chloride, sodium bromide and sodium nitrate, whereas largely underestimating the sorption coefficient associated with sodium perchlorate. For both concentrations considered (i.e., 0.1 mol/L and 0.2 mol/L) the deviations of Donnan exclusion prediction from experimentally measured salt sorption coefficients are 85% and 62% for sodium chloride, -31% and -4% for sodium bromide, -40% and -12% for sodium nitrate. However, for sodium perchlorate, the deviations can be as large as -540% and -850%, associated with 0.1 mol/L and 0.2 mol/L solutions, respectively. It is then questionable that the anomalously high sorption coefficient of sodium perchlorate only owe to its large bare anion radius and large anion excess polarizability.

Perchlorate based salts such as lithium perchlorate and sodium perchlorate were reported to be dissolved in high-molecular-weight poly (ethylene oxide) (PEO) to yield solid polyelectrolytes for fuel cell or battery applications.[32, 33, 56-58] In these studies, sodium perchlorate was believed to form complex structure with the repeating ethylene oxide (EO) groups in solid PEO through coordinate bond, as shown in Figure 13.[33, 57]

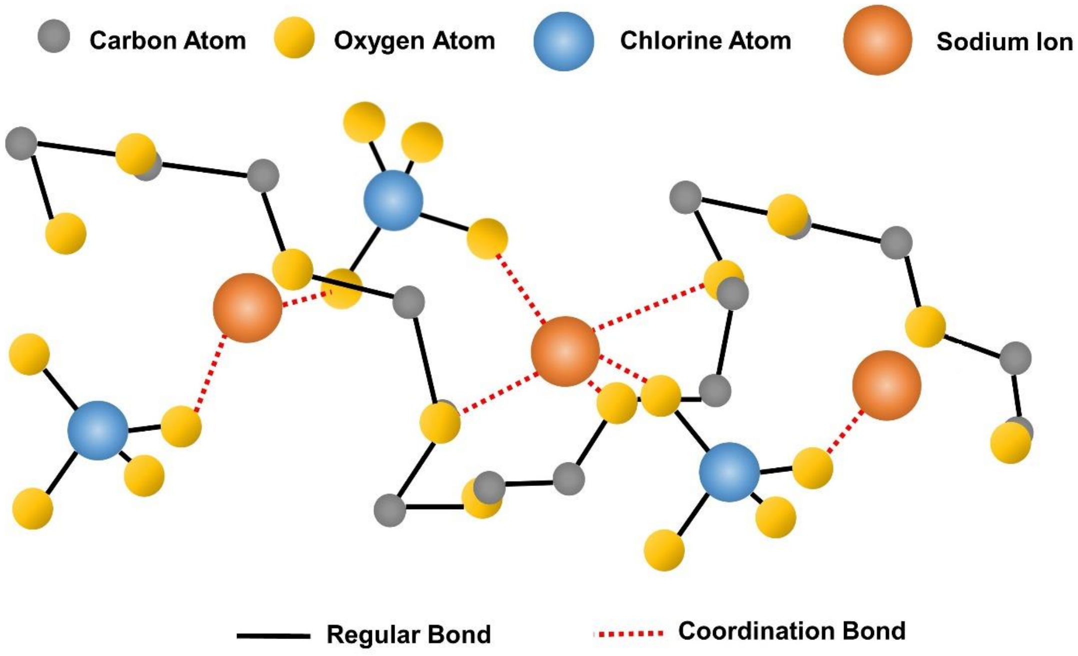

Figure 14. Schematic illustration of solid $NaClO_4$-PEO complexation crystalline structure.[33]

It was then conjectured that sodium perchlorate could also form complex structure with the EO groups in hydrated polymer, when at least 3 repeating EO units (4 oxygen atoms) were presented. Such hypothesis was tested by measuring the salt sorption coefficients of XLPEGDA (n=3), XLPEGDA (n=10) and XLPEGDA (n=13) and comparing their salt sorption coefficients K_s with their water sorption coefficients K_w, as presented in Figure 15. The salt sorption coefficients K_s of XLPEGDA (n=3), XLPEGDA (n=10) and XLPEGDA (n=13) all follow the trend: $K_{\mathrm{NaClO_4}} \gg K_{\mathrm{NaNO_3}} > K_{\mathrm{NaBr}} > K_{\mathrm{NaCl}}$, which is qualitatively consistent with the trend observed with XLAMPS. Particularly, for XLPEGDA (n=10) and XLPEGDA (n=13), their sodium perchlorate sorption coefficient are extremely high such that their $K_{\mathrm{NaClO_4}}$ exceed the K_w values. For non-charged, hydrated polymer membranes, K_w was commonly regarded as an upper limit for K_s.[38, 43] When K_s exceeds K_w, the salt concentration in the membrane solution (i.e., mol salt in membrane phase / L water in membrane phase) will also exceed the concentration of the external solution. This phenomena indicates that salt in membrane not only dissolve in membrane water phase, but also somewhat dissolve in membrane polymer matrix, indicating a preferential interaction.[39] Therefore, for XLPEGDA (n=10) and XLPEGDA (n=13), it is highly possible that a substantial amount of sodium perchlorate dissolved in their polymer matrix through the formation of $NaClO_4$-EO complex structure, thus resulting anomalously high $K_{\mathrm{NaClO_4}}$. Besides, since PEGDA (n=10) is also presented in the structure of XLAMPS as crosslinker, it is highly possible that such $NaClO_4$-EO complex also formed in the interaction between sodium perchlorate and XLAMPS, thus also contributing to the high $K_{\mathrm{NaClO_4}}$ of XLAMPS.

However, it is unclear whether the $NaClO_4$-EO complex can also form in XLPEGDA (n=3). Theoretically, XLPEGDA (n=3) with three repeating EO units along with an oxygen atom, (Figure 4) should just satisfy the requirement for forming the complex structure. Whereas the sodium perchlorate sorption coefficient of XLPEGDA (n=3), though much higher than the sorption coefficients of other three salts, is still far below K_w. In that case, it might be arbitrary to draw solid conclusion about whether sodium perchlorate dissolved in the membrane matrix through $NaClO_4$-EO complex or not. Future work needs to be done to investigate this issue. Our present conjecture is that $NaClO_4$-EO complex can form in XLPEGDA (n=3), but probably only in small amount. The choice of experimental sorption coefficients for Figure 13 was also based on such conjecture. Compared with XLAMPS, XLPEGDA (n=10) and XLPEGDA (n=13), the impacts of $NaClO_4$-EO structure seemed to be minimized on XLPEGDA (n=3). Its sorption coefficients, therefore better represents only the electrostatic effects and dispersion effects, and are then taken to compare with theoretical calculation.

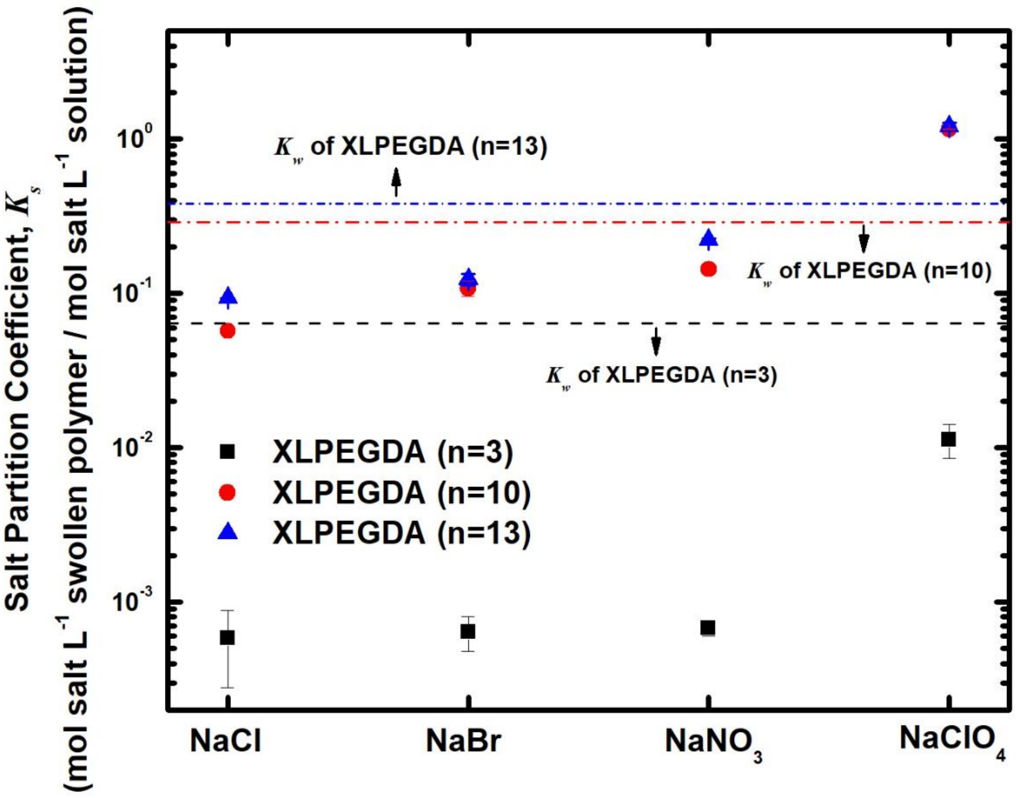

Figure 15. Comparison between salt sorption coefficient K_s and water sorption coefficient K_w of XLPEGDA (n=3,10,13) membranes. K_s was measured with 0.1 mol/L salt solutions. K_w was measured with 0.1 mol/L salt solutions as well.

3.5 Salt (Co-ion) Diffusion

The salt diffusion coefficients in XLAMPS were measured with the four salts, to investigate their contributions to membrane permselectivity as well. The salt diffusion coefficients in membrane were measured though desorption, after the membrane sample was equilibrated with 0.2 mol/L salt solutions. The ratio of diffusion coefficients of salt in membrane phase D_s^m to diffusion coefficients D_s^s in aqueous bulk solution were calculated and compared with the prediction of Mackie and Mears model, as presented in Figure 16.

Mackie and Meares model is a relatively simple, but widely applied model to predict the salt diffusion coefficient in swollen, homogenous polymeric membrane. The basic assumption of this model is that the whole membrane system is composed of an internal solution and a polymer matrix, and the presence of the polymer matrix reduces the cross-sectional area available for transport and introduces tortuosity,[29] thus slowing diffusion relative to bulk solution properties. Therefore, the increase in polymer water content reduces the effect of this transport resistance.[9, 31] According to this model, salt diffusion occurs in membrane solution phase and there is no interactions between diffusing salts and polymeric membrane. Therefore, the salt diffusion coefficients in membrane only depends on the water volume fraction of the membrane, and bulk solution diffusion coefficient, as shown in equation 15:

$$D_s^m = D_s^s \left(\frac{K_w}{2-K_w}\right)^2 \tag{15}$$

where: D_s^s was taken to be the salt diffusion coefficients in aqueous solution, at infinite dilution, 298.15K in this study.[53, 59]

It was revealed in Figure 16 that the Mackie and Meares model provided relatively good estimation of D_s^m/D_s^s for sodium nitrate and sodium bromide. The D_s^m/D_s^s values of those two salts are statistically indistinguishable with each other (0.11±0.007 for sodium bromide compared to 0.10±0.017 for sodium nitrate) and statistically indistinguishable with the value predicted by Mackie and Meares model (0.118). The D_s^m/D_s^s of sodium chloride falls slightly above the Mackie and Meares model's prediction. (0.13±0.006 as compared to 0.118) Whereas the D_s^m/D_s^s of sodium perchlorate falls far below the prediction (0.04±0.005 as compared to 0.118). Although Mackie and Meares model contains no explicitly ion-related parameters, it implicitly accounts for ion diffusion behaviors through the incorporation of D_s^s into the equation.

Therefore, for sodium bromide and sodium nitrate, the consistency between their experimental D_s^m/D_s^s and Mackie and Meares model predictions indicates that their diffusion behaviors in membrane phase are somewhat predictable from their diffusion behaviors in bulk solution. Whereas the inconsistent situation of sodium chloride and sodium perchlorate, indicates that their membrane diffusion behaviors are not completely predictable from their bulk solution diffusion behaviors.

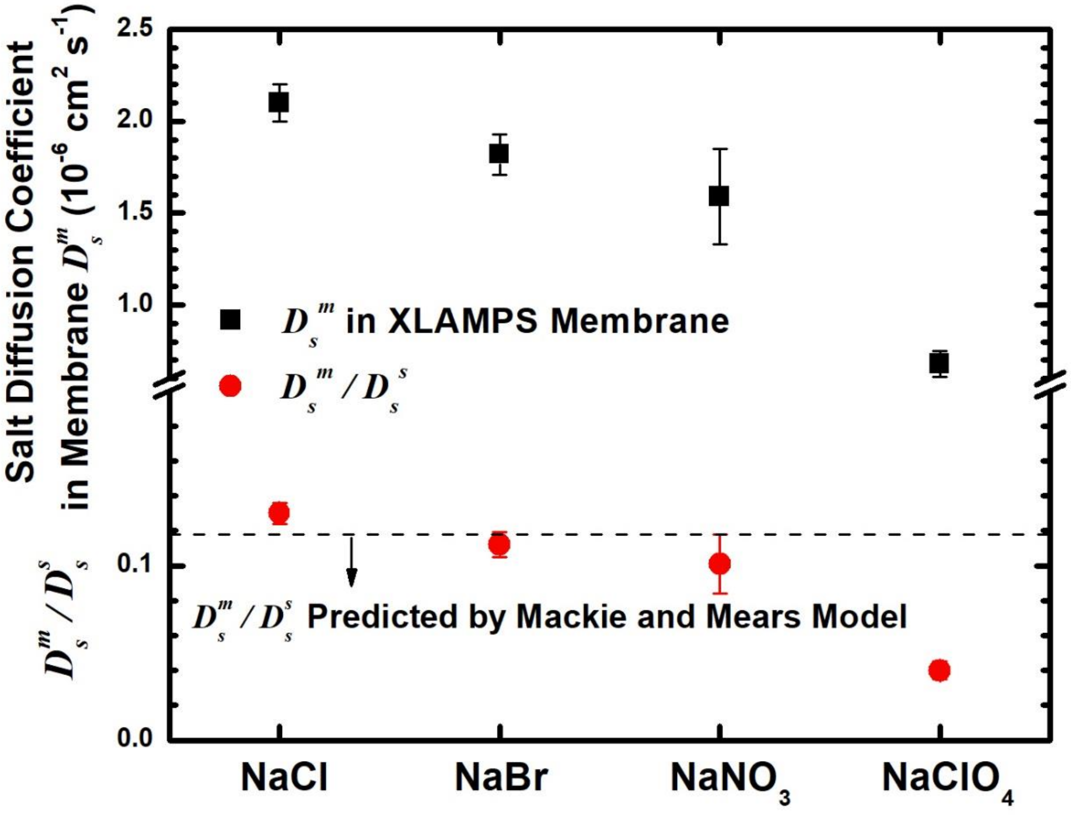

Figure 16. Salt diffusion coefficient D_s^m of XLAMPS membrane and D_s^m/D_s^s for different salts. D_s^m was measured through desorption after the membrane sample was equilibrated with 0.2 mol/L salt solutions. D_s^s was calculated from the diffusivity of cations and anions, in aqueous solutions at infinite dilution, 298.15K through the relationship $D_s^s = \frac{2D_s^+D_s^-}{D_s^+ + D_s^-}$.[53, 59]

In most liquid-based diffusion coefficient models, such as Stokes-Einstein and Wilke and Chang equation, solute size is believed to inversely correlated with solute diffusion coefficient.[17] It is then reasonable to assume that the diffusion coefficient of ion is inversely correlated with the ion size, and ion hydrated radius might be the best option to represent ion size in bulk solution.[60, 61] The hydrated anion radius of four salts were presented in Table 4, as well as the bulk diffusion coefficients of the four salts. In Table 4, sodium chloride with smallest hydrated anion radius, showed highest diffusion coefficient, whereas sodium perchlorate, with largest hydrated anion radius, showed lowest diffusion coefficient. An inverse correlation seems to exist between hydrated anion size and salt diffusion coefficient.

Table 4 Hydrated anion radius[58] and bulk solution diffusion coefficients of the four salts considered in this study.

Salt	Hydrated Anion Radius in Aqueous Phase (**Å**)	Salt Diffusion Coefficient in Aqueous Solution, at Infinite Dilution, at 298.15K (10^{-5} cm^2 s^{-1})
NaCl	3.32	1.61
NaBr	3.30	1.63
$NaNO_3$	3.35	1.57
$NaClO_4$	3.38	1.53

Back to the discussion with regard to Mackie and Meares prediction, for sodium bromide and sodium nitrate, their diffusion coefficients in membrane are predictable from their diffusion coefficients in bulk solution, and their relative magnitude of diffusion coefficient in bulk solution is controlled by the difference in their hydrated anion radius. Therefore, for sodium bromide and sodium nitrate, co-ion hydrated radii is probably the main factor that affects their diffusion coefficient in membrane. However, for sodium chloride and sodium perchlorate, their diffusion coefficients in membrane are not completely predictable from their diffusion coefficients in bulk solution, indicating other interactions might be going on. For sodium chloride, that interaction might be a weak repulsive force between polymer and diffusing salts. Such repulsive force might distance sodium chloride from polymer matrix, thus reducing diffusing resistance and ultimately increasing diffusion coefficient. For sodium perchlorate, that interaction might be a strong attractive force between polymer and diffusing salts. Such attractive force might immobilize sodium perchlorate on polymer matrix, thus greatly reducing its diffusion coefficient. Combining with previous discussion about $NaClO_4$-EO complexation, it is highly possible that the $NaClO_4$-EO complex structure can act as the immobilization mechanism. However, more work needs to be conducted to figure out the issue with sodium chloride and sodium perchlorate.

4. Conclusions

Three origins of uncertainty in the apparent permselectivity measurement were firstly discussed: temperature variations, concentration deviations, and membrane potential measurement fluctuations. Apparent permselectivity decreased by approximately 2% as temperature increased from 14 to 31^{o}C. This uncertainty, however, was of comparable magnitude to the replicate uncertainty. Second, membrane potential measurement fluctuations were found to contribute likely 0.2% to 0.5% uncertainty to the apparent permselectivity measurement. Finally, the influence of solution preparation errors were found to be the smallest contributor of apparent permselectivity uncertainty (approximately 0.015% to 0.1%). The low concentration solution is more sensitive to salt concentration deviations than the high concentration solution.

The permselectivity, salt sorption coefficients and salt diffusion coefficients of XLAMPS were characterized with four salts, sodium chloride, sodium bromide, sodium nitrate and sodium perchlorate to investigate the co-ion specific effects on membrane permselectiviy. The cation was fixed as sodium, and anions were all associated with different bare ion radius and excess polarizability. The permselectivity of XLAMPS was demonstrated to be different when different co-ions were used, and followed the trend: $\alpha_{\mathrm{NaCl}} > \alpha_{\mathrm{NaNO_3}} > \alpha_{\mathrm{NaBr}} > \alpha_{\mathrm{NaClO_4}}$. The salt sorption coefficients of XLAMPS followed the trend: $K_{\mathrm{NaClO_4}} > K_{\mathrm{NaNO_3}} > K_{\mathrm{NaBr}} > K_{\mathrm{NaCl}}$. The salt diffusion coefficients in XLAMPS followed the opposite trend with sorption coefficients, in the way that $D^m_{\mathrm{NaCl}} > D^m_{\mathrm{NaBr}} > D^m_{\mathrm{NaNO_3}} > D^m_{\mathrm{NaClO_4}}$. The opposite trend, combined with permselectivity results, revealed a competing mechanism between co-ion sorption and co-ion diffusion, in determining permselectivity.

A theoretical model, was proposed to connect co-ion bare radius and co-ion excess polarizability with co-ion sorption coefficient. According to this model, large bare co-ion radius and large co-ion polarizability were related with low co-ion sorption free energy barrier, thus high co-ion sorption coefficient. The calculated total energy barrier followed the trend: $\Delta G_{NaCl}^{Total} > \Delta G_{NaBr}^{Total} > \Delta G_{\mathrm{NaNO_3}}^{Total} > \Delta G_{\mathrm{NaClO_4}}^{Total}$. The free energy was then also calculated using experimental data with XLPEGDA (n=3), and also showed the trend: $\Delta G_{NaCl}^{Exp} > \Delta G_{NaBr}^{Exp} > \Delta G_{\mathrm{NaNO_3}}^{Exp} > \Delta G_{\mathrm{NaClO_4}}^{Exp}$. The consistency between calculation and experimental results demonstrated the qualitative validity of this model. Larger co-ion bare radius and excess polarizability tended to result in higher co-ion sorption coefficient. Besides, the formation of ion-polymer complexation could also be an origin of high co-ion sorption coefficient, and this phenomena was observed for sodium perchlorate with XLAMPS. The anomalously high sorption coefficients of $NaClO_4$ with XLAMPS, XLPEGDA (n=10) and XLPEGDA (n=13) were also believed to also result from the formation of $NaClO_4$-EO complexation.

The membrane diffusion coefficients of sodium bromide and sodium nitrate, are predictable from their diffusion coefficients in bulk solution, through Mackie and Meares model. Therefore their diffusion coefficients in membrane is inversely correlated with their co-ion hydrated radii. The membrane diffusion coefficients of sodium chloride is slightly larger than Mackie and Meares model prediction, which might indicates a weak repulsive effects between sodium chloride and polymer matrix. The membrane diffusion coefficients of sodium perchlorate is anomalously lower than Mackie and Meares model prediction, which might indicates an strong attractive effects between sodium perchlorate and polymer matrix, and it is highly possible that the formation of $NaClO_4$-EO complexation is responsible for such strong attractive effects.

5. References

[1] Kamcev, J.; Freeman, B. D. Charged Polymer Membranes for Environmental/Energy Applications. *Annual Review of Chemical and Biomolecular Engineering* **2016,** *7*, 111-33.

[2] Cusick, R. D.; Kim, Y.; Logan, B. E. Energy Capture from Thermolytic Solutions in Microbial Reverse-Electrodialysis Cells. *Science* **2012,** *335* (6075), 1474-1477.

[3] Logan, B. E.; Elimelech, M. Membrane-based processes for sustainable power generation using water. *Nature* **2012,** *488* (7411), 313-9.

[4] Ramon, G. Z.; Feinberg, B. J.; Hoek, E. M. Membrane-based production of salinity-gradient power. *Energy & environmental science* **2011,** *4* (11), 4423-4434.

[5] McGinnis, R. L.; McCutcheon, J. R.; Elimelech, M. A novel ammonia–carbon dioxide osmotic heat engine for power generation. *Journal of Membrane Science* **2007,** *305* (1-2), 13-19.

[6] Długołęcki, P.; Gambier, A.; Nijmeijer, K.; Wessling, M. Practical Potential of Reverse Electrodialysis As Process for Sustainable Energy Generation. *Environmental Science & Technology* **2009,** *43* (17), 6888-6894.

[7] Post, J. W.; Veerman, J.; Hamelers, H. V. M.; Euverink, G. J. W.; Metz, S. J.; Nymeijer, K.; Buisman, C. J. N. Salinity-gradient power: Evaluation of pressure-retarded osmosis and reverse electrodialysis. *Journal of Membrane Science* **2007,** *288* (1-2), 218-230.

[8] Geise, G. M.; Lee, H.-S.; Miller, D. J.; Freeman, B. D.; McGrath, J. E.; Paul, D. R. Water purification by membranes: The role of polymer science. *Journal of Polymer Science Part B: Polymer Physics* **2010,** *48* (15), 1685-1718.

[9] Geise, G. M.; Paul, D. R.; Freeman, B. D. Fundamental water and salt transport properties of polymeric materials. *Progress in Polymer Science* **2014,** *39* (1), 1-42.

[10] Strathmann, H.; Giorno, L.; Drioli, E., *Introduction to membrane science and technology*. Wiley-VCH Weinheim: 2011; Vol. 544.

[11] Strathmann, H.; Grabowski, A.; Eigenberger, G. Ion-exchange membranes in the chemical process industry. *Industrial & Engineering Chemistry Research* **2013,** *52* (31), 10364-10379.

[12] Veerman, J.; Saakes, M.; Metz, S. J.; Harmsen, G. J. Reverse electrodialysis: A validated process model for design and optimization. *Chemical Engineering Journal* **2011,** *166* (1), 256-268.

[13] Dlugolecki, P.; Nymeijer, K.; Metz, S.; Wessling, M. Current status of ion exchange membranes for power generation from salinity gradients. *Journal of Membrane Science* **2008,** *319* (1-2), 214-222.

[14] Geise, G. M.; Hickner, M. A.; Logan, B. E. Ionic Resistance and Permselectivity Tradeoffs in Anion Exchange Membranes. *ACS Applied Materials & Interfaces* **2013,** *5* (20), 10294-10301.

[15] Strathmann, H. Electrodialysis, a mature technology with a multitude of new applications. *Desalination* **2010,** *264* (3), 268-288.

[16] Ghyselbrecht, K.; Huygebaert, M.; Van der Bruggen, B.; Ballet, R.; Meesschaert, B.; Pinoy, L. Desalination of an industrial saline water with conventional and bipolar membrane electrodialysis. *Desalination* **2013,** *318,* 9-18.

[17] Cussler, E. L., *Diffusion: mass transfer in fluid systems*. Cambridge university press: 2009.

[18] Deen, W. M., *Analysis of Transport Phenomena, Topics in Chemical Engineering*. Oxford University Press, New York: 1998; Vol. 3.

[19] Kamcev, J.; Paul, D. R.; Freeman, B. D. Effect of fixed charge group concentration on equilibrium ion sorption in ion exchange membranes. *Journal of Materials Chemistry A* **2017,** *5* (9), 4638-4650.

[20] Kamcev, J.; Paul, D. R.; Manning, G. S.; Freeman, B. D. Predicting Salt Permeability Coefficients in Highly Swollen, Highly Charged Ion Exchange Membranes. *ACS Applied Materials & Interfaces* **2017,** *9* (4), 4044-4056.

[21] Geise, G. M.; Cassady, H. J.; Paul, D. R.; Logan, B. E.; Hickner, M. A. Specific ion effects on membrane potential and the permselectivity of ion exchange membranes. *Physical Chemistry Chemical Physics* **2014,** *16* (39), 21673-81.

[22] Imteyaz, S. Effects of monovalent ions on membrane potential and permselectivity: evaluation of fixed charge density of polymer based zirconium aluminophosphate composite membrane. *RSC Advances* **2015,** *5* (116), 96008-96018.

[23] Cassady, H. J.; Cimino, E. C.; Kumar, M.; Hickner, M. A. Specific ion effects on the permselectivity of sulfonated poly (ether sulfone) cation exchange membranes. *Journal of Membrane Science* **2016,** *508*, 146-152.

[24] Avci, A. H.; Sarkar, P.; Tufa, R. A.; Messana, D.; Argurio, P.; Fontananova, E.; Di Profio, G.; Curcio, E. Effect of Mg 2+ ions on energy generation by Reverse Electrodialysis. *Journal of Membrane Science* **2016,** *520*, 499-506.

[25] Logan, B. E.; Elimelech, M. Membrane-based processes for sustainable power generation using water. *Nature* **2012,** *488* (7411), 313-319.

[26] Weber, A. Z.; Mench, M. M.; Meyers, J. P.; Ross, P. N.; Gostick, J. T.; Liu, Q. Redox flow batteries: a review. *Journal of Applied Electrochemistry* **2011,** *41* (10), 1137.

[27] Marcus, Y., *Ion properties*. CRC Press: 1997; Vol. 1.

[28] Parsegian, A. Energy of an ion crossing a low dielectric membrane: solutions to four relevant electrostatic problems. *Nature* **1969,** *221* (5183), 844-846.

[29] Mackie, J.; Meares, P. In *The diffusion of electrolytes in a cation-exchange resin membrane. I. Theoretical*, Proceedings of the Royal Society of London A: Mathematical, Physical and Engineering Sciences, The Royal Society: 1955; pp 498-509.

[30] Mackie, J.; Meares, P. In *The diffusion of electrolytes in a cation-exchange resin membrane. II. Experimental,* Proceedings of the Royal Society of London A: Mathematical, Physical and Engineering Sciences, The Royal Society: 1955; pp 510-518.

[31] Zhang, H.; Geise, G. M. Modeling the water permeability and water/salt selectivity tradeoff in polymer membranes. *Journal of Membrane Science* **2016,** *520*, 790-800.

[32] Andreev, Y. G.; Bruce, P. G. Polymer electrolyte structure and its implications. *Electrochimica Acta* **2000,** *45* (8), 1417-1423.

[33] Lightfoot, P.; Mehta, M. A.; Bruce, P. G. Structure of the poly (ethylene oxide)–sodium perchlorate complex PEO 3–NaClO 4 from powder X-ray diffraction data. *Journal of Materials Chemistry* **1992,** *2* (4), 379-381.

[34] Miyoshi, H.; Chubachi, M.; Yamagami, M.; Kataoka, T. Characteristic coefficients for equilibrium between solution and Neosepta or Selemion cation exchange membranes. *Journal of Chemical and Engineering Data* **1992,** *37* (1), 120-124.

[35] Sato, K. Effects of the stripping solution concentrations on the separation degree in Donnan dialysis for binary systems of amino acids. *Journal of Membrane Science* **2008,** *309* (1), 175-181.

[36] Ju, H.; McCloskey, B. D.; Sagle, A. C.; Kusuma, V. A.; Freeman, B. D. Preparation and characterization of crosslinked poly (ethylene glycol) diacrylate hydrogels as fouling-resistant membrane coating materials. *Journal of Membrane Science* **2009,** *330* (1), 180-188.

[37] Geise, G. M.; Falcon, L. P.; Freeman, B. D.; Paul, D. R. Sodium chloride sorption in sulfonated polymers for membrane applications. *Journal of Membrane Science* **2012,** *423–424*, 195-208.

[38] Ju, H.; Sagle, A. C.; Freeman, B. D.; Mardel, J. I.; Hill, A. J. Characterization of sodium chloride and water transport in crosslinked poly (ethylene oxide) hydrogels. *Journal of Membrane Science* **2010,** *358* (1), 131-141.

[39] Mettler Toledo. Density Knit: http://www.mt.com/in/en/home/library/operating-instructions/laboratory-weighing/NC_density_OI/jcr:content/download/file/file.res/Operating_Instructions_Density%20Kit_(OP-EN).pdf. (Access Date: 10 July 2017)

[40] Cruise, G. M.; Scharp, D. S.; Hubbell, J. A. Characterization of permeability and network structure of interfacially photopolymerized poly (ethylene glycol) diacrylate hydrogels. *Biomaterials* **1998,** *19* (14), 1287-1294.

[41] Pitzer, K. S.; Mayorga, G. Thermodynamics of electrolytes. II. Activity and osmotic coefficients for strong electrolytes with one or both ions univalent. *The Journal of Physical Chemistry* **1973,** *77* (19), 2300-2308.

[42] Ku, H. Notes on the use of propagation of error formulas. *Journal of Research of the National Bureau of Standards* **1966,** *70* (4).

[43] Yasuda, H.; Lamaze, C.; Ikenberry, L. Permeability of solutes through hydrated polymer membranes. Part I. Diffusion of sodium chloride. *Macromolecular Chemistry and Physics* **1968,** *118* (1), 19-35.

[44] Crank, J., *The mathematics of diffusion*. Oxford university press: 1979.

[45] Donnan, F. G. The theory of membrane equilibria. *Chemical Reviews* **1924,** *1* (1), 73-90.

[46] Kamcev, J.; Paul, D. R.; Freeman, B. D. Ion activity coefficients in ion exchange polymers: applicability of Manning's counterion condensation theory. *Macromolecules* **2015,** *48* (21), 8011-8024.

[47] Duignan, T. T.; Parsons, D. F.; Ninham, B. W. A continuum model of solvation energies including electrostatic, dispersion, and cavity contributions. *The Journal of Physical Chemistry B* **2013,** *117* (32), 9421-9429.

[48] Boström, M.; Ninham, B. Energy of an ion crossing a low dielectric membrane: the role of dispersion self-free energy. *Biophysical chemistry* **2005,** *114* (2), 95-101.

[49] Tavares, F. W.; Bratko, D.; Blanch, H. W.; Prausnitz, J. M. Ion-Specific Effects in the Colloid− Colloid or Protein− Protein Potential of Mean Force: Role of Salt− Macroion van der Waals Interactions. *The Journal of Physical Chemistry B* **2004,** *108* (26), 9228-9235.

[50] Anderson, J.; Pusch, W. The Membrane/Water Partition Coefficients of Ions: Electrostatic Calculations of Dielectric Heterogeneity. *Berichte der Bunsengesellschaft für physikalische Chemie* **1976,** *80* (9), 846-849.

[51] Yaroshchuk, A. E. Dielectric exclusion of ions from membranes. *Advances in colloid and interface science* **2000,** *85* (2), 193-230.

[52] Mahanty, J.; Ninham, B. W., *Dispersion forces*. Academic Press London: 1976; Vol. 5.

[53] Haynes, W. M., *CRC handbook of chemistry and physics*. CRC press: 2014.

[54] Kunz, W.; Belloni, L.; Bernard, O.; Ninham, B. W. Osmotic coefficients and surface tensions of aqueous electrolyte solutions: role of dispersion forces. *The Journal of Physical Chemistry B* **2004,** *108* (7), 2398-2404.

[55] Dagastine, R. R.; Prieve, D. C.; White, L. R. The dielectric function for water and its application to van der Waals forces. *Journal of colloid and interface science* **2000,** *231* (2), 351-358.

[56] Fullerton-Shirey, S. K.; Maranas, J. K. Effect of LiClO4 on the structure and mobility of PEO-based solid polymer electrolytes. *Macromolecules* **2009,** *42* (6), 2142-2156.

[57] Bruce, P. G. Structure and electrochemistry of polymer electrolytes. *Electrochimica acta* **1995,** *40* (13-14), 2077-2085.

[58] Feng, S.; Shi, D.; Liu, F.; Zheng, L.; Nie, J.; Feng, W.; Huang, X.; Armand, M.; Zhou, Z. Single lithium-ion conducting polymer electrolytes based on poly [(4-styrenesulfonyl)(trifluoromethanesulfonyl) imide] anions. *Electrochimica Acta* **2013,** *93*, 254-263.

[59] Deen, W. M. Analysis of transport phenomena. **2012**.

[60] Nightingale Jr, E. Phenomenological theory of ion solvation. Effective radii of hydrated ions. *The Journal of Physical Chemistry* **1959,** *63* (9), 1381-1387.

[61] Marcus, Y. Effect of ions on the structure of water: structure making and breaking. *Chemical reviews* **2009,** *109* (3), 1346-1370.